Pose-Tracking Without Linear and Angular Velocity Feedback Using Dual Quaternions

Nuno Filipe, Alfredo Valverde, and Panagiotis Tsiotras, *Senior Member, IEEE*

***Abstract*—Since vision-based sensors typically cannot directly measure the relative linear and angular velocities between two spacecraft, it is useful to develop attitude- and position-tracking controllers, namely, pose-tracking controllers, that do not require such measurements. Using dual quaternions and based on an existing attitude-only tracking controller, a pose-tracking controller that does not require relative linear or angular velocity measurements is developed in this paper. Compared to existing literature, this velocity-free pose-tracking controller guarantees that the pose of the chaser spacecraft will converge to the desired pose independently of the initial state, even if the reference motion is not sufficiently exciting. In addition, the convergence region does not depend on the gains chosen by the user. The velocity-free controller is verified and compared with a velocity-feedback controller through two simulations. In particular, the proposed velocity-free controller is compared qualitatively and quantitatively with a velocity-feedback controller and an EKF using a relatively realistic satellite proximity operation scenario.**

***Index Terms*—Spacecraft proximity operations, pose tracking, dual quaternions, velocity-free, vision sensors.**

NOMENCLATURE

$0_{m\times n}$	m-by-n matrix of zeros.
$I_{n\times n}$	n-by-n identity matrix.
$\mathtt{1}$	Quaternion $(1, 0_{3\times 1})$.
$\mathtt{0}$	Quaternion $(0, 0_{3\times 1})$.
$q_{\text{Y/Z}}$	Unit quaternion from the Z-frame to the Y-frame.
$\bar{\omega}^{\text{X}}_{\text{Y/Z}}$	Angular velocity of the Y-frame with respect to the Z-frame expressed in the X-frame.
$\bar{v}^{\text{X}}_{\text{Y/Z}}$	Linear velocity of the origin of the Y-frame with respect to the Z-frame expressed in the X-frame.
$\bar{r}^{\text{X}}_{\text{Y/Z}}$	Translation vector from the origin of the Z-frame to the origin of the Y-frame expressed in the X-frame.
$\bar{\tau}^{\text{B}}$	Total external moment vector applied to the body about its center of mass expressed in the body frame.
$\bar{f}^{\text{B}}$	Total external force vector applied to the body expressed in the body frame.
$\mathbf{1}$	Dual quaternion $\mathtt{1} + \epsilon\mathtt{0}$.
$\mathbf{0}$	Dual quaternion $\mathtt{0} + \epsilon\mathtt{0}$.
$\boldsymbol{q}_{\text{Y/Z}}$	Unit dual quaternion from the Z-frame to the Y-frame.
$\boldsymbol{\omega}^{\text{X}}_{\text{Y/Z}}$	Dual velocity of the Y-frame with respect to the Z-frame expressed in the X-frame.
$\boldsymbol{f}^{\text{B}}$	Total external dual force applied to the body about its center of mass expressed in the body frame.
M^{B}	Dual inertia matrix.
$\boldsymbol{f}^{\text{B}}_{c}$	Dual control force expressed in the body frame.

Manuscript received Month DD, YYYY; revised Month DD, YYYY. This work was supported by the International Fulbright Science and Technology Award sponsored by the Bureau of Educational and Cultural Affairs (ECA) of the U.S. Department of State and AFRL research award FA9453-13-C-0201.

The authors are with the Daniel Guggenheim School of Aerospace Engineering, Georgia Institute of Technology, Atlanta, GA 30332-0150 USA (e-mail: {nuno.filipe,avalverde3,tsiotras}@gatech.edu).

I. INTRODUCTION

THE term proximity operations has been widely used in recent years to describe a wide range of space missions that require a spacecraft to remain close to another space object. Such missions include, for example, the inspection, health monitoring, surveillance, servicing, and refueling of a space asset by another spacecraft. One of the biggest challenges in autonomous space proximity operations, either cooperative or uncooperative, is the need to autonomously and accurately track time-varying relative position and attitude references, i.e., pose references, with respect to a moving target, in order to avoid on-orbit collisions and achieve the overall mission goals. In addition, if the target spacecraft is uncooperative, the Guidance, Navigation, and Control (GNC) system of the chaser spacecraft must not rely on any help from the target spacecraft. In this case, vision-based sensors, such as cameras, are typically used to measure the relative pose between the spacecraft. Although vision-based sensors have several attractive properties, they introduce new challenges, such as no direct linear and angular velocity measurements.

Velocity-free pose-tracking controllers have been proposed by several authors. In particular, in [1], a velocity-free pose-tracking controller that does not require mass and inertia matrix information is proposed. However, as explained in [2], if the reference pose is not sufficiently exciting, the pose of the body might not converge to the desired pose. In [3], another velocity-free pose-tracking controller is designed based on the vectrix formalism. This controller suffers from two problems. First, the attitude of the body cannot be more than 180 deg away from the desired attitude. Second, the region of convergence is dependent on the gains chosen by the user. In other words, an arbitrarily large region of convergence requires arbitrarily large gains. In turn, high gains may lead to actuator saturation and poor noise rejection. Finally, in [4], it is shown that a locally asymptotically stable closed-loop system can be obtained by combining an almost globally asymptotically stable attitude-only tracking controller with a locally exponentially convergent angular velocity observer. Although the theory presented in [4] can, in principle, be extended to pose control, only attitude control is demonstrated.

Compared to existing literature, the velocity-free pose-tracking controller presented in this paper is almost globally asymptotically stable. In particular, the pose of the body converges to the desired pose independently of the initial condition and, unlike in [1], the reference motion does not need to be exciting. Moreover, the region of convergence does not depend on the gains chosen by the user. Note that "almost" global stability means stability for all initial conditions, except for a set of measure zero as a result of topological obstructions [5]. In that sense, almost global stability is the strongest type of stability one can hope for using continuous controllers for this system.

As in the recent papers [6]–[8], the analogies between quaternions and dual quaternions are explored to develop the controller proposed in this paper. Dual quaternions are built on, and are an extension of, classical quaternions. They provide a compact representation of not only the attitude, but also of the position of a frame with respect to another frame. Their properties, including examples of previous applications, are discussed in length in [7]. However, the property that makes dual quaternions most appealing is that the combined translational and rotational kinematic and dynamic equations of motion written in terms of dual quaternions have the same form as the rotational-only kinematic and dynamic equations of motion written in terms of quaternions (albeit the operations have now to be interpreted in *dual* quaternion algebra). As a consequence, as shown in [6], [7], pose controllers with certain properties can be developed from existing attitude-only controllers with analogous properties by (almost) just replacing quaternions by dual quaternions. Following the same idea, in this paper a velocity-free pose-tracking controller is developed based on the attitude-tracking controller of [9] that guarantees almost global asymptotic stability of the attitude-tracking error when angular velocity measurements are not available.

This paper is organized as follows. In Section II, the main operations and properties of quaternions and dual quaternions are reviewed. Then, a pose-tracking controller that requires relative linear and angular velocity measurements is derived in Section III. Based on this velocity-feedback controller, the velocity-free controller is derived in Section IV. Subsequently, both controllers are verified numerically in Section V. Two examples are presented. In the first example, a chaser spacecraft is required to track an elliptical motion around a target satellite while pointing at it. In the second example, the velocity-free controller is compared qualitatively and quantitatively to the velocity-feedback controller fed with velocity estimates produced by an EKF through a more realistic satellite proximity operations simulation.

II. Mathematical Preliminaries

For the benefit of the reader, the main properties of quaternions and dual quaternions are summarized in this section. For additional information, the reader is referred to [7], [8], [10].

A. Quaternions

A quaternion can be represented as an ordered pair $q = (q_0, \bar{q})$, where $\bar{q} = [q_1 \ q_2 \ q_3]^\intercal \in \mathbb{R}^3$ is the *vector part* of the quaternion and $q_0 \in \mathbb{R}$ is the *scalar part*. Henceforth, quaternions with zero scalar part and with zero vector part will be referred to as *vector quaternions* and *scalar quaternions*, respectively. The sets of quaternions, vector quaternions, and scalar quaternions will be denoted by $\mathbb{H} = \{q : \ q = (q_0, \bar{q}),\ \bar{q} \in \mathbb{R}^3,\ q_0 \in \mathbb{R}\}$, $\mathbb{H}^v = \{q \in \mathbb{H} : \ q_0 = 0\}$, and $\mathbb{H}^s = \{q \in \mathbb{H} : \ \bar{q} = 0_{3\times 1}\}$, respectively. The elementary operations on quaternions are given by:

$$\text{Addition: } a + b = (a_0 + b_0, \bar{a} + \bar{b}) \in \mathbb{H},$$
$$\text{Multiplication by a scalar: } \lambda a = (\lambda a_0, \lambda \bar{a}) \in \mathbb{H},$$
$$\text{Multiplication: } ab = (a_0 b_0 - \bar{a} \cdot \bar{b}, a_0 \bar{b} + b_0 \bar{a} + \bar{a} \times \bar{b}) \in \mathbb{H},$$
$$\text{Conjugation: } a^* = (a_0, -\bar{a}) \in \mathbb{H},$$
$$\text{Dot product: } a \cdot b = (a_0 b_0 + \bar{a} \cdot \bar{b}, 0_{3\times 1}) \in \mathbb{H}^s,$$
$$\text{Cross product: } a \times b = (0, b_0 \bar{a} + a_0 \bar{b} + \bar{a} \times \bar{b}) \in \mathbb{H}^v,$$
$$\text{Norm: } \|a\|^2 = aa^* = a^* a = a \cdot a = (a_0^2 + \bar{a} \cdot \bar{a}, 0_{3\times 1}) \in \mathbb{H}^s,$$
$$\text{Scalar part: } \mathrm{sc}(a) = (a_0, 0_{3\times 1}) \in \mathbb{H}^s,$$
$$\text{Vector part: } \mathrm{vec}(a) = (0, \bar{a}) \in \mathbb{H}^v,$$
$$\text{Multiplication by a matrix: } M * a = (M_{11} a_0 + M_{12} \bar{a}, \ M_{21} a_0 + M_{22} \bar{a}) \in \mathbb{H},$$

where $a, b \in \mathbb{H}$, $\lambda \in \mathbb{R}$, $0_{m\times n}$ is a m-by-n matrix of zeros,

$$M = \begin{bmatrix} M_{11} & M_{12} \\ M_{21} & M_{22} \end{bmatrix} \in \mathbb{R}^{4\times 4},$$

$M_{11} \in \mathbb{R}$, $M_{12} \in \mathbb{R}^{1\times 3}$, $M_{21} \in \mathbb{R}^{3\times 1}$, and $M_{22} \in \mathbb{R}^{3\times 3}$. Note that $ab \neq ba$, in general. In this paper, the quaternions $(1, \bar{0})$ and $(0, \bar{0})$ will be denoted by $\mathtt{1}$ and $\mathtt{0}$, respectively. The following properties follow from the previous definitions [10]: $a \cdot (bc) = b \cdot (ac^*) = c \cdot (b^* a)$, $\|ab\| = \|a\|\|b\|$, and $(M * a) \cdot b = a \cdot (M^\intercal * b)$, where $a, b, c \in \mathbb{H}$ and $M \in \mathbb{R}^{4\times 4}$. The $\mathcal{L}_\infty$-norm of a function $u : [0, \infty) \to \mathbb{H}$ is defined as $\|u\|_\infty = \sup_{t\geq 0} \|u(t)\|$. Moreover, the function $u \in \mathcal{L}_\infty$, if and only if $\|u\|_\infty < \infty$.

The relative orientation of a body frame with respect to an inertial frame can be represented by the *unit quaternion* $q_{\text{B/I}} = (\cos(\frac{\phi}{2}), \sin(\frac{\phi}{2})\bar{n})$, where the body frame is said to be rotated with respect to the inertial frame about the unit vector $\bar{n}$ (i.e., $\bar{n} \cdot \bar{n}$=1) by an angle ϕ. The quaternion $q_{\text{B/I}}$ is a unit quaternion because it belongs to the set $\mathbb{H}^u = \{q \in \mathbb{H} : \ q \cdot q = 1\}$. The body coordinates of a vector, $\bar{v}^{\text{B}}$, can be calculated from the inertial coordinates of that same vector, $\bar{v}^{\text{I}}$, and vice-versa, through $v^{\text{B}} = q_{\text{B/I}}^* v^{\text{I}} q_{\text{B/I}}$ and $v^{\text{I}} = q_{\text{B/I}} v^{\text{B}} q_{\text{B/I}}^*$, where $v^{\text{X}} = (0, \bar{v}^{\text{X}})$.

The rotational kinematic equations of the body frame and of a frame with some desired orientation, both with respect to the inertial frame and represented by the unit quaternions $q_{\text{B/I}}$ and $q_{\text{D/I}}$, respectively, are given by $\dot{q}_{\text{B/I}} = \frac{1}{2} q_{\text{B/I}} \omega_{\text{B/I}}^{\text{B}} = \frac{1}{2} \omega_{\text{B/I}}^{\text{I}} q_{\text{B/I}}$ and $\dot{q}_{\text{D/I}} = \frac{1}{2} q_{\text{D/I}} \omega_{\text{D/I}}^{\text{D}} = \frac{1}{2} \omega_{\text{D/I}}^{\text{I}} q_{\text{D/I}}$, where $\omega_{\text{Y/Z}}^{\text{X}} = (0, \bar{\omega}_{\text{Y/Z}}^{\text{X}})$ and $\bar{\omega}_{\text{Y/Z}}^{\text{X}} = [p_{\text{Y/Z}}^{\text{X}}, q_{\text{Y/Z}}^{\text{X}}, r_{\text{Y/Z}}^{\text{X}}]^\intercal$ is the angular velocity of the Y-frame with respect to the Z-frame expressed in the X-frame. The error quaternion $q_{\text{B/D}} = q_{\text{D/I}}^* q_{\text{B/I}}$ is the unit quaternion that rotates the desired frame onto the body frame. By differentiating $q_{\text{B/D}}$ the kinematic equations of the error quaternion turn out to be

$$\dot{q}_{\text{B/D}} = \frac{1}{2} q_{\text{B/D}} \omega_{\text{B/D}}^{\text{B}} = \frac{1}{2} \omega_{\text{B/D}}^{\text{D}} q_{\text{B/D}}, \tag{1}$$

where $\omega_{\text{B/D}}^{\text{B}} = \omega_{\text{B/I}}^{\text{B}} - \omega_{\text{D/I}}^{\text{B}}$ (and $\omega_{\text{B/D}}^{\text{D}} = \omega_{\text{B/I}}^{\text{D}} - \omega_{\text{D/I}}^{\text{D}}$).

B. Dual Quaternions

A dual quaternion is defined as $\boldsymbol{q} = q_r + \epsilon q_d$, where $q_r, q_d \in \mathbb{H}$ are the *real* and *dual part* of the dual quaternion, respectively, and ϵ is the *dual unit* defined as $\epsilon^2 = 0$ and $\epsilon \neq 0$. Hereafter, dual quaternions with $q_r, q_d \in \mathbb{H}^v$ and with $q_r, q_d \in \mathbb{H}^s$ will be referred to as *dual vector quaternions* and *dual scalar quaternions*, respectively. The sets of dual quaternions, dual scalar quaternions, and dual vector quaternions will be denoted by $\mathbb{H}_d = \{\boldsymbol{q} : \ \boldsymbol{q} = q_r + \epsilon q_d, \ q_r, q_d \in \mathbb{H}\}$, $\mathbb{H}_d^s = \{\boldsymbol{q} : \ \boldsymbol{q} = q_r + \epsilon q_d, \ q_r, q_d \in \mathbb{H}^s\}$, and $\mathbb{H}_d^v = \{\boldsymbol{q} : \boldsymbol{q} = q_r + \epsilon q_d, \ q_r, q_d \in \mathbb{H}^v\}$, respectively. Moreover, the set of dual scalar quaternions with zero dual part will be denoted by $\mathbb{H}_d^r = \{\boldsymbol{q} : \ \boldsymbol{q} = q_r + \epsilon(\bar{0}, 0), \ q_r \in \mathbb{H}^s\}$. The elementary operations on dual quaternions are given by:

$$\text{Addition: } \boldsymbol{a} + \boldsymbol{b} = (a_r + b_r) + \epsilon(a_d + b_d) \in \mathbb{H}_d,$$
$$\text{Multiplication by a scalar: } \lambda\boldsymbol{a} = (\lambda a_r) + \epsilon(\lambda a_d) \in \mathbb{H}_d,$$
$$\text{Multiplication: } \boldsymbol{a}\boldsymbol{b} = (a_r b_r) + \epsilon(a_r b_d + a_d b_r) \in \mathbb{H}_d,$$
$$\text{Conjugation: } \boldsymbol{a}^* = a_r^* + \epsilon a_d^* \in \mathbb{H}_d,$$
$$\text{Swap: } \boldsymbol{a}^{\mathsf{S}} = a_d + \epsilon a_r \in \mathbb{H}_d,$$
$$\text{Dot product: } \boldsymbol{a} \cdot \boldsymbol{b} = a_r \cdot b_r + \epsilon(a_d \cdot b_r + a_r \cdot b_d) \in \mathbb{H}_d^s,$$
$$\text{Cross product: } \boldsymbol{a} \times \boldsymbol{b} = a_r \times b_r + \epsilon(a_d \times b_r + a_r \times b_d) \in \mathbb{H}_d^v,$$
$$\text{Circle product: } \boldsymbol{a} \circ \boldsymbol{b} = a_r \cdot b_r + a_d \cdot b_d \in \mathbb{H}_d^r,$$
$$\text{Dual norm: } \|\boldsymbol{a}\|_d^2 = (a_r \cdot a_r) + \epsilon(2a_r \cdot a_d) \in \mathbb{H}_d^s,$$
$$\text{Norm: } \|\boldsymbol{a}\|^2 = \boldsymbol{a} \circ \boldsymbol{a} \in \mathbb{H}_d^r,$$
$$\text{Scalar part: } \mathrm{sc}\big(\boldsymbol{a}\big) = \mathrm{sc}\big(a_r\big) + \epsilon\,\mathrm{sc}\big(a_d\big) \in \mathbb{H}_d^s,$$
$$\text{Vector part: } \mathrm{vec}\big(\boldsymbol{a}\big) = \mathrm{vec}\big(a_r\big) + \epsilon\,\mathrm{vec}\big(a_d\big) \in \mathbb{H}_d^v,$$
$$\text{Multiplication by a matrix: } M \star \boldsymbol{q} = (M_{11} * q_r + M_{12} * q_d) + \epsilon(M_{21} * q_r + M_{22} * q_d) \in \mathbb{H}_d,$$

where $\boldsymbol{a}, \boldsymbol{b} \in \mathbb{H}_d$, $\lambda \in \mathbb{R}$,

$$M = \begin{bmatrix} M_{11} & M_{12} \\ M_{21} & M_{22} \end{bmatrix}, \quad M_{11}, M_{12}, M_{21}, M_{22} \in \mathbb{R}^{4\times 4}.$$

Note that $\boldsymbol{a}\boldsymbol{b} \neq \boldsymbol{b}\boldsymbol{a}$, in general. In this paper, the dual quaternions $1 + \epsilon 0$ and $0 + \epsilon 0$ will be denoted by $\mathbf{1}$ and $\mathbf{0}$, respectively. The following properties follow from the previous definitions [6], [10]:

$$\boldsymbol{a} \circ (\boldsymbol{b}\boldsymbol{c}) = \boldsymbol{b}^{\mathsf{S}} \circ (\boldsymbol{a}^{\mathsf{S}}\boldsymbol{c}^*) = \boldsymbol{c}^{\mathsf{S}} \circ (\boldsymbol{b}^*\boldsymbol{a}^{\mathsf{S}}), \quad \boldsymbol{a}, \boldsymbol{b}, \boldsymbol{c} \in \mathbb{H}_d, \tag{2}$$
$$\boldsymbol{a} \circ (\boldsymbol{b} \times \boldsymbol{c}) = \boldsymbol{b}^{\mathsf{S}} \circ (\boldsymbol{c} \times \boldsymbol{a}^{\mathsf{S}}) = \boldsymbol{c}^{\mathsf{S}} \circ (\boldsymbol{a}^{\mathsf{S}} \times \boldsymbol{b}), \quad \boldsymbol{a}, \boldsymbol{b}, \boldsymbol{c} \in \mathbb{H}_d^v, \tag{3}$$
$$\boldsymbol{a} \times \boldsymbol{a} = 0, \quad \boldsymbol{a} \in \mathbb{H}_d^v, \tag{4}$$
$$\boldsymbol{a} \times \boldsymbol{b} = -\boldsymbol{b} \times \boldsymbol{a}, \quad \boldsymbol{a}, \boldsymbol{b} \in \mathbb{H}_d^v, \tag{5}$$
$$\boldsymbol{a}^{\mathsf{S}} \circ \boldsymbol{b}^{\mathsf{S}} = \boldsymbol{a} \circ \boldsymbol{b}, \quad \boldsymbol{a}, \boldsymbol{b} \in \mathbb{H}_d, \tag{6}$$
$$\|\boldsymbol{a}^{\mathsf{S}}\| = \|\boldsymbol{a}\|, \quad \boldsymbol{a} \in \mathbb{H}_d, \tag{7}$$
$$\|\boldsymbol{a}^*\| = \|\boldsymbol{a}\|, \quad \boldsymbol{a} \in \mathbb{H}_d, \tag{8}$$
$$(M \star \boldsymbol{a}) \circ \boldsymbol{b} = \boldsymbol{a} \circ (M^{\mathsf{T}} \star \boldsymbol{b}), \ \boldsymbol{a}, \boldsymbol{b} \in \mathbb{H}_d, \ M \in \mathbb{R}^{8\times 8}, \tag{9}$$
$$|\boldsymbol{a} \circ \boldsymbol{b}| \leq \|\boldsymbol{a}\|\|\boldsymbol{b}\|, \quad \boldsymbol{a}, \boldsymbol{b} \in \mathbb{H}_d, \tag{10}$$
$$\|\boldsymbol{a}\boldsymbol{b}\| \leq \sqrt{3/2}\,\|\boldsymbol{a}\|\|\boldsymbol{b}\|, \ \boldsymbol{a}, \boldsymbol{b} \in \mathbb{H}_d. \tag{11}$$

The $\mathcal{L}_\infty$-norm of a function $\boldsymbol{u} : [0, \infty) \to \mathbb{H}_d$ is defined as $\|\boldsymbol{u}\|_\infty = \sup_{t\geq 0} \|\boldsymbol{u}(t)\|$. Moreover, the function $\boldsymbol{u} \in \mathcal{L}_\infty$, if and only if $\|\boldsymbol{u}\|_\infty < \infty$.

A compact way to represent the pose of a body frame with respect to an inertial frame is through the *unit dual quaternion* $\boldsymbol{q}_{\text{B/I}} = q_{\text{B/I}} + \epsilon\frac{1}{2} r^{\text{I}}_{\text{B/I}} q_{\text{B/I}} = q_{\text{B/I}} + \epsilon\frac{1}{2} q_{\text{B/I}} r^{\text{B}}_{\text{B/I}}$, where $\bar{r}^{\text{X}}_{\text{Y/Z}} = [x^{\text{X}}_{\text{Y/Z}} \ y^{\text{X}}_{\text{Y/Z}} \ z^{\text{X}}_{\text{Y/Z}}]^{\mathsf{T}}$ and $\bar{r}^{\text{X}}_{\text{Y/Z}}$ is the translation vector from the origin of the Z-frame to the origin of the Y-frame expressed in the X-frame. The dual quaternion $\boldsymbol{q}_{\text{B/I}}$ is a unit dual quaternion because it belongs to the set $\mathbb{H}_d^u = \{\boldsymbol{q} \in \mathbb{H}_d : \ \boldsymbol{q} \cdot \boldsymbol{q} = \boldsymbol{q}\boldsymbol{q}^* = \boldsymbol{q}^*\boldsymbol{q} = \|\boldsymbol{q}\|_d = 1\}$.

The rotational and translational kinematic equations of the body frame and of a frame with some desired pose, both with respect to the inertial frame and represented by the unit dual quaternions $\boldsymbol{q}_{\text{B/I}}$ and $\boldsymbol{q}_{\text{D/I}} = q_{\text{D/I}} + \epsilon\frac{1}{2} r^{\text{I}}_{\text{D/I}} q_{\text{D/I}} = q_{\text{D/I}} + \epsilon\frac{1}{2} q_{\text{D/I}} r^{\text{D}}_{\text{D/I}}$, respectively, are given by $\dot{\boldsymbol{q}}_{\text{B/I}} = \frac{1}{2}\boldsymbol{\omega}^{\text{I}}_{\text{B/I}}\boldsymbol{q}_{\text{B/I}} = \frac{1}{2}\boldsymbol{q}_{\text{B/I}}\boldsymbol{\omega}^{\text{B}}_{\text{B/I}}$ and $\dot{\boldsymbol{q}}_{\text{D/I}} = \frac{1}{2}\boldsymbol{\omega}^{\text{I}}_{\text{D/I}}\boldsymbol{q}_{\text{D/I}} = \frac{1}{2}\boldsymbol{q}_{\text{D/I}}\boldsymbol{\omega}^{\text{D}}_{\text{D/I}}$, where $\boldsymbol{\omega}^{\text{X}}_{\text{Y/Z}}$ is the *dual velocity* of the Y-frame with respect to the Z-frame expressed in the X-frame, $\boldsymbol{\omega}^{\text{X}}_{\text{Y/Z}} = \omega^{\text{X}}_{\text{Y/Z}} + \epsilon(v^{\text{X}}_{\text{Y/Z}} + \omega^{\text{X}}_{\text{Y/Z}} \times r^{\text{X}}_{\text{X/Y}})$, $v^{\text{X}}_{\text{Y/Z}} = (0, \bar{v}^{\text{X}}_{\text{Y/Z}})$, and $\bar{v}^{\text{X}}_{\text{Y/Z}} = [u^{\text{X}}_{\text{Y/Z}} \ v^{\text{X}}_{\text{Y/Z}} \ w^{\text{X}}_{\text{Y/Z}}]^{\mathsf{T}}$ is the linear velocity of the origin of the Y-frame with respect to the Z-frame expressed in the X-frame.

By direct analogy to the error quaternion, the *dual error quaternion* is defined as $\boldsymbol{q}_{\text{B/D}} = \boldsymbol{q}^*_{\text{D/I}}\boldsymbol{q}_{\text{B/I}} = q_{\text{B/D}} + \epsilon\frac{1}{2} q_{\text{B/D}} r^{\text{B}}_{\text{B/D}} = q_{\text{B/D}} + \epsilon\frac{1}{2} r^{\text{D}}_{\text{B/D}} q_{\text{B/D}}$. The dual error quaternion is the unit dual quaternion that represents the pose of the body frame with respect to the desired frame. By differentiating $\boldsymbol{q}_{\text{B/D}}$, the kinematic equations of the dual error quaternion turn out to be

$$\dot{\boldsymbol{q}}_{\text{B/D}} = \tfrac{1}{2}\boldsymbol{q}_{\text{B/D}}\boldsymbol{\omega}^{\text{B}}_{\text{B/D}} = \tfrac{1}{2}\boldsymbol{\omega}^{\text{D}}_{\text{B/D}}\boldsymbol{q}_{\text{B/D}}, \tag{12}$$

where $\boldsymbol{\omega}^{\text{B}}_{\text{B/D}} = \boldsymbol{\omega}^{\text{B}}_{\text{B/I}} - \boldsymbol{\omega}^{\text{B}}_{\text{D/I}}$, $\boldsymbol{\omega}^{\text{B}}_{\text{D/I}} = \boldsymbol{q}^*_{\text{B/D}}\boldsymbol{\omega}^{\text{D}}_{\text{D/I}}\boldsymbol{q}_{\text{B/D}}$, and $\boldsymbol{\omega}^{\text{D}}_{\text{B/I}} = \boldsymbol{q}_{\text{B/D}}\boldsymbol{\omega}^{\text{B}}_{\text{B/I}}\boldsymbol{q}^*_{\text{B/D}}$. Note that (12) has the same form as (1).

The dual quaternion representation of the relative rotational and translational dynamic equations of a rigid body are given by

$$(\dot{\boldsymbol{\omega}}^{\text{B}}_{\text{B/D}})^{\mathsf{S}} = (M^{\text{B}})^{-1} \star \Big(\boldsymbol{f}^{\text{B}} - (\boldsymbol{\omega}^{\text{B}}_{\text{B/D}} + \boldsymbol{\omega}^{\text{B}}_{\text{D/I}}) \times \big(M^{\text{B}} \star ((\boldsymbol{\omega}^{\text{B}}_{\text{B/D}})^{\mathsf{S}} + (\boldsymbol{\omega}^{\text{B}}_{\text{D/I}})^{\mathsf{S}}) \big) - M^{\text{B}} \star (\boldsymbol{q}^*_{\text{B/D}}\dot{\boldsymbol{\omega}}^{\text{D}}_{\text{D/I}}\boldsymbol{q}_{\text{B/D}})^{\mathsf{S}} - M^{\text{B}} \star (\boldsymbol{\omega}^{\text{B}}_{\text{D/I}} \times \boldsymbol{\omega}^{\text{B}}_{\text{B/D}})^{\mathsf{S}} \Big), \tag{13}$$

where $\boldsymbol{f}^{\text{B}} = f^{\text{B}} + \epsilon\tau^{\text{B}}$ is the total external *dual force* applied to the body about its center of mass expressed in the body frame, $f^{\text{B}} = (0, \bar{f}^{\text{B}})$, $\bar{f}^{\text{B}} = [f^{\text{B}}_1 \ f^{\text{B}}_2 \ f^{\text{B}}_3]^{\mathsf{T}}$ is the total external force vector applied to the body expressed in the body frame, $\tau^{\text{B}} = (0, \bar{\tau}^{\text{B}})$, and $\bar{\tau}^{\text{B}} = [\tau^{\text{B}}_1 \ \tau^{\text{B}}_2 \ \tau^{\text{B}}_3]^{\mathsf{T}}$ is the total external moment vector applied to the body about its center of mass expressed in the body frame. Finally, $M^{\text{B}} \in \mathbb{R}^{8\times 8}$ is the *dual inertia matrix* defined as

$$M^{\text{B}} = \begin{bmatrix} 1 & 0_{1\times 3} & 0 & 0_{1\times 3} \\ 0_{3\times 1} & mI_{3\times 3} & 0_{3\times 1} & 0_{3\times 3} \\ 0 & 0_{1\times 3} & 1 & 0_{1\times 3} \\ 0_{3\times 1} & 0_{3\times 3} & 0_{3\times 1} & \bar{I}^{\text{B}} \end{bmatrix}, \ I^{\text{B}} = \begin{bmatrix} 1 & 0_{1\times 3} \\ 0_{3\times 1} & \bar{I}^{\text{B}} \end{bmatrix},$$

$\bar{I}^{\text{B}} \in \mathbb{R}^{3\times 3}$ is the mass moment of inertia of the body about its center of mass written in the body frame, and m is the mass of the body. Note that M^{B} is a symmetric positive-definite matrix. Also note the similarity between (13) and the quaternion representation of the relative rotational(-only) dynamic equations given by $\dot{\omega}^{\text{B}}_{\text{B/D}} = (I^{\text{B}})^{-1} * (\tau^{\text{B}} - (\omega^{\text{B}}_{\text{B/D}} + \omega^{\text{B}}_{\text{D/I}}) \times (I^{\text{B}} * (\omega^{\text{B}}_{\text{B/D}} + \omega^{\text{B}}_{\text{D/I}})) - I^{\text{B}} * (q^*_{\text{B/D}}\dot{\omega}^{\text{D}}_{\text{D/I}}q_{\text{B/D}}) - I^{\text{B}} * (\omega^{\text{B}}_{\text{D/I}} \times \omega^{\text{B}}_{\text{B/D}}))$.

III. Velocity-Feedback Pose-Tracking Controller

When the relative linear and angular velocities are known, the controller proposed in Theorem 1 below can be used to track a time-varying reference pose.

Theorem 1: Consider the rigid body relative kinematic and dynamic equations (12) and (13), respectively. Let the total external dual force acting on the rigid body be defined by the feedback control law

$$\boldsymbol{f}^{\mathrm{B}} = -k_p \mathrm{vec}\big(\boldsymbol{q}^*_{\mathrm{B/D}}(\boldsymbol{q}^{\mathsf{s}}_{\mathrm{B/D}} - \mathbf{1}^{\mathsf{s}})\big) - k_d(\boldsymbol{\omega}^{\mathrm{B}}_{\mathrm{B/D}})^{\mathsf{s}} + M^{\mathrm{B}} \star (\boldsymbol{q}^*_{\mathrm{B/D}} \dot{\boldsymbol{\omega}}^{\mathrm{D}}_{\mathrm{D/I}} \boldsymbol{q}_{\mathrm{B/D}})^{\mathsf{s}} + \boldsymbol{\omega}^{\mathrm{B}}_{\mathrm{D/I}} \times (M^{\mathrm{B}} \star (\boldsymbol{\omega}^{\mathrm{B}}_{\mathrm{D/I}})^{\mathsf{s}}), \quad k_p, k_d > 0, \tag{14}$$

and assume that $\dot{\boldsymbol{\omega}}^{\mathrm{D}}_{\mathrm{D/I}}, \boldsymbol{\omega}^{\mathrm{D}}_{\mathrm{D/I}} \in \mathcal{L}_\infty$. Then, $\boldsymbol{q}_{\mathrm{B/D}} \to \pm\mathbf{1}$ (i.e., $q_{\mathrm{B/D}} \to \pm 1$ and $r^{\mathrm{B}}_{\mathrm{B/D}} \to 0$) and $\boldsymbol{\omega}^{\mathrm{B}}_{\mathrm{B/D}} \to \mathbf{0}$ (i.e., $\omega^{\mathrm{B}}_{\mathrm{B/D}} \to 0$ and $v^{\mathrm{B}}_{\mathrm{B/D}} \to 0$) as $t \to +\infty$ for all initial conditions.

Proof: First, note that $\boldsymbol{q}_{\mathrm{B/D}} = \pm\mathbf{1}$ and $\boldsymbol{\omega}^{\mathrm{B}}_{\mathrm{B/D}} = \mathbf{0}$ are in fact the equilibrium conditions for the closed-loop system formed by (12), (13), and (14). Consider now the following candidate Lyapunov function for the equilibrium point $\boldsymbol{q}_{\mathrm{B/D}} = +\mathbf{1}$ and $\boldsymbol{\omega}^{\mathrm{B}}_{\mathrm{B/D}} = \mathbf{0}$ (equivalently, $(\boldsymbol{\omega}^{\mathrm{B}}_{\mathrm{B/D}})^{\mathsf{s}} = \mathbf{0}$): $V(\boldsymbol{q}_{\mathrm{B/D}}, \boldsymbol{\omega}^{\mathrm{B}}_{\mathrm{B/D}}) = k_p(\boldsymbol{q}_{\mathrm{B/D}} - \mathbf{1}) \circ (\boldsymbol{q}_{\mathrm{B/D}} - \mathbf{1}) + \frac{1}{2}(\boldsymbol{\omega}^{\mathrm{B}}_{\mathrm{B/D}})^{\mathsf{s}} \circ (M^{\mathrm{B}} \star (\boldsymbol{\omega}^{\mathrm{B}}_{\mathrm{B/D}})^{\mathsf{s}})$. Note that V is a valid candidate Lyapunov function since $V(\boldsymbol{q}_{\mathrm{B/D}} = \mathbf{1}, \boldsymbol{\omega}^{\mathrm{B}}_{\mathrm{B/D}} = \mathbf{0}) = 0$ and $V(\boldsymbol{q}_{\mathrm{B/D}}, \boldsymbol{\omega}^{\mathrm{B}}_{\mathrm{B/D}}) > 0$ for all $(\boldsymbol{q}_{\mathrm{B/D}}, \boldsymbol{\omega}^{\mathrm{B}}_{\mathrm{B/D}}) \in \mathbb{H}^u_d \times \mathbb{H}^v_d \backslash \{\mathbf{1}, \mathbf{0}\}$. The time derivative of V is equal to $\dot{V} = 2k_p(\boldsymbol{q}_{\mathrm{B/D}} - \mathbf{1}) \circ \dot{\boldsymbol{q}}_{\mathrm{B/D}} + (\boldsymbol{\omega}^{\mathrm{B}}_{\mathrm{B/D}})^{\mathsf{s}} \circ (M^{\mathrm{B}} \star (\dot{\boldsymbol{\omega}}^{\mathrm{B}}_{\mathrm{B/D}})^{\mathsf{s}})$. Then, by plugging in (12) and (13) and using (3), it follows that $\dot{V} = (\boldsymbol{\omega}^{\mathrm{B}}_{\mathrm{B/D}})^{\mathsf{s}} \circ (k_p \boldsymbol{q}^*_{\mathrm{B/D}}(\boldsymbol{q}^{\mathsf{s}}_{\mathrm{B/D}} - \mathbf{1}^{\mathsf{s}}) + \boldsymbol{f}^{\mathrm{B}} - (\boldsymbol{\omega}^{\mathrm{B}}_{\mathrm{B/D}} + \boldsymbol{\omega}^{\mathrm{B}}_{\mathrm{D/I}}) \times (M^{\mathrm{B}} \star ((\boldsymbol{\omega}^{\mathrm{B}}_{\mathrm{B/D}})^{\mathsf{s}} + (\boldsymbol{\omega}^{\mathrm{B}}_{\mathrm{D/I}}))^{\mathsf{s}} - M^{\mathrm{B}} \star (\boldsymbol{q}^*_{\mathrm{B/D}} \dot{\boldsymbol{\omega}}^{\mathrm{D}}_{\mathrm{D/I}} \boldsymbol{q}_{\mathrm{B/D}})^{\mathsf{s}} - M^{\mathrm{B}} \star (\boldsymbol{\omega}^{\mathrm{B}}_{\mathrm{D/I}} \times \boldsymbol{\omega}^{\mathrm{B}}_{\mathrm{B/D}})^{\mathsf{s}})$. Introducing the feedback control law (14) yields $\dot{V} = (\boldsymbol{\omega}^{\mathrm{B}}_{\mathrm{B/D}})^{\mathsf{s}} \circ (-k_d(\boldsymbol{\omega}^{\mathrm{B}}_{\mathrm{B/D}})^{\mathsf{s}}) + (\boldsymbol{\omega}^{\mathrm{B}}_{\mathrm{B/D}})^{\mathsf{s}} \circ (k_p \boldsymbol{q}^*_{\mathrm{B/D}}(\boldsymbol{q}^{\mathsf{s}}_{\mathrm{B/D}} - \mathbf{1}^{\mathsf{s}}) - k_p \mathrm{vec}\big(\boldsymbol{q}^*_{\mathrm{B/D}}(\boldsymbol{q}^{\mathsf{s}}_{\mathrm{B/D}} - \mathbf{1}^{\mathsf{s}})\big)) + (\boldsymbol{\omega}^{\mathrm{B}}_{\mathrm{B/D}})^{\mathsf{s}} \circ (-(\boldsymbol{\omega}^{\mathrm{B}}_{\mathrm{B/D}} + \boldsymbol{\omega}^{\mathrm{B}}_{\mathrm{D/I}}) \times (M^{\mathrm{B}} \star ((\boldsymbol{\omega}^{\mathrm{B}}_{\mathrm{B/D}})^{\mathsf{s}} + (\boldsymbol{\omega}^{\mathrm{B}}_{\mathrm{D/I}}))^{\mathsf{s}}) - M^{\mathrm{B}} \star (\boldsymbol{\omega}^{\mathrm{B}}_{\mathrm{D/I}} \times \boldsymbol{\omega}^{\mathrm{B}}_{\mathrm{B/D}})^{\mathsf{s}} + \boldsymbol{\omega}^{\mathrm{B}}_{\mathrm{D/I}} \times (M^{\mathrm{B}} \star (\boldsymbol{\omega}^{\mathrm{B}}_{\mathrm{D/I}})^{\mathsf{s}}))$. Note that the second term is zero because it is the circle product of a dual vector quaternion with a dual scalar quaternion. Moreover, the third term can be shown to be equal to zero as follows: $(\boldsymbol{\omega}^{\mathrm{B}}_{\mathrm{B/D}})^{\mathsf{s}} \circ (-(\boldsymbol{\omega}^{\mathrm{B}}_{\mathrm{B/D}} + \boldsymbol{\omega}^{\mathrm{B}}_{\mathrm{D/I}}) \times (M^{\mathrm{B}} \star ((\boldsymbol{\omega}^{\mathrm{B}}_{\mathrm{B/D}})^{\mathsf{s}} + (\boldsymbol{\omega}^{\mathrm{B}}_{\mathrm{D/I}}))^{\mathsf{s}}) - M^{\mathrm{B}} \star (\boldsymbol{\omega}^{\mathrm{B}}_{\mathrm{D/I}} \times \boldsymbol{\omega}^{\mathrm{B}}_{\mathrm{B/D}})^{\mathsf{s}} + \boldsymbol{\omega}^{\mathrm{B}}_{\mathrm{D/I}} \times (M^{\mathrm{B}} \star (\boldsymbol{\omega}^{\mathrm{B}}_{\mathrm{D/I}})^{\mathsf{s}})) = ((\boldsymbol{\omega}^{\mathrm{B}}_{\mathrm{B/I}})^{\mathsf{s}} - (\boldsymbol{\omega}^{\mathrm{B}}_{\mathrm{D/I}})^{\mathsf{s}}) \circ (-\boldsymbol{\omega}^{\mathrm{B}}_{\mathrm{B/I}} \times (M^{\mathrm{B}} \star (\boldsymbol{\omega}^{\mathrm{B}}_{\mathrm{B/I}})^{\mathsf{s}}) - M^{\mathrm{B}} \star (\boldsymbol{\omega}^{\mathrm{B}}_{\mathrm{D/I}} \times (\boldsymbol{\omega}^{\mathrm{B}}_{\mathrm{B/I}} - \boldsymbol{\omega}^{\mathrm{B}}_{\mathrm{D/I}}))^{\mathsf{s}} + \boldsymbol{\omega}^{\mathrm{B}}_{\mathrm{D/I}} \times (M^{\mathrm{B}} \star (\boldsymbol{\omega}^{\mathrm{B}}_{\mathrm{D/I}})^{\mathsf{s}})) = (\boldsymbol{\omega}^{\mathrm{B}}_{\mathrm{B/I}})^{\mathsf{s}} \circ (-\boldsymbol{\omega}^{\mathrm{B}}_{\mathrm{B/I}} \times (M^{\mathrm{B}} \star (\boldsymbol{\omega}^{\mathrm{B}}_{\mathrm{B/I}})^{\mathsf{s}}) - M^{\mathrm{B}} \star (\boldsymbol{\omega}^{\mathrm{B}}_{\mathrm{D/I}} \times \boldsymbol{\omega}^{\mathrm{B}}_{\mathrm{B/I}})^{\mathsf{s}} + \boldsymbol{\omega}^{\mathrm{B}}_{\mathrm{D/I}} \times (M^{\mathrm{B}} \star (\boldsymbol{\omega}^{\mathrm{B}}_{\mathrm{D/I}})^{\mathsf{s}})) - (\boldsymbol{\omega}^{\mathrm{B}}_{\mathrm{D/I}})^{\mathsf{s}} \circ (-\boldsymbol{\omega}^{\mathrm{B}}_{\mathrm{B/I}} \times (M^{\mathrm{B}} \star (\boldsymbol{\omega}^{\mathrm{B}}_{\mathrm{B/I}})^{\mathsf{s}}) - M^{\mathrm{B}} \star (\boldsymbol{\omega}^{\mathrm{B}}_{\mathrm{D/I}} \times \boldsymbol{\omega}^{\mathrm{B}}_{\mathrm{B/I}})^{\mathsf{s}} + \boldsymbol{\omega}^{\mathrm{B}}_{\mathrm{D/I}} \times (M^{\mathrm{B}} \star (\boldsymbol{\omega}^{\mathrm{B}}_{\mathrm{D/I}})^{\mathsf{s}})) = -(\boldsymbol{\omega}^{\mathrm{B}}_{\mathrm{B/I}})^{\mathsf{s}} \circ (\boldsymbol{\omega}^{\mathrm{B}}_{\mathrm{B/I}} \times (M^{\mathrm{B}} \star (\boldsymbol{\omega}^{\mathrm{B}}_{\mathrm{B/I}})^{\mathsf{s}})) - (\boldsymbol{\omega}^{\mathrm{B}}_{\mathrm{B/I}})^{\mathsf{s}} \circ (M^{\mathrm{B}} \star (\boldsymbol{\omega}^{\mathrm{B}}_{\mathrm{D/I}} \times \boldsymbol{\omega}^{\mathrm{B}}_{\mathrm{B/I}})^{\mathsf{s}}) + (\boldsymbol{\omega}^{\mathrm{B}}_{\mathrm{B/I}})^{\mathsf{s}} \circ (\boldsymbol{\omega}^{\mathrm{B}}_{\mathrm{D/I}} \times (M^{\mathrm{B}} \star (\boldsymbol{\omega}^{\mathrm{B}}_{\mathrm{D/I}})^{\mathsf{s}})) + (\boldsymbol{\omega}^{\mathrm{B}}_{\mathrm{D/I}})^{\mathsf{s}} \circ (\boldsymbol{\omega}^{\mathrm{B}}_{\mathrm{B/I}} \times (M^{\mathrm{B}} \star (\boldsymbol{\omega}^{\mathrm{B}}_{\mathrm{B/I}})^{\mathsf{s}})) + (\boldsymbol{\omega}^{\mathrm{B}}_{\mathrm{D/I}})^{\mathsf{s}} \circ (M^{\mathrm{B}} \star (\boldsymbol{\omega}^{\mathrm{B}}_{\mathrm{D/I}} \times \boldsymbol{\omega}^{\mathrm{B}}_{\mathrm{B/I}})^{\mathsf{s}}) - (\boldsymbol{\omega}^{\mathrm{B}}_{\mathrm{D/I}})^{\mathsf{s}} \circ (\boldsymbol{\omega}^{\mathrm{B}}_{\mathrm{D/I}} \times (M^{\mathrm{B}} \star (\boldsymbol{\omega}^{\mathrm{B}}_{\mathrm{D/I}})^{\mathsf{s}}))$. Note that the first and last terms are zero due to (3) and (4). Moreover, using (6) and (9), the second and fifth terms can be rewritten as $-(M^{\mathrm{B}} \star (\boldsymbol{\omega}^{\mathrm{B}}_{\mathrm{B/I}})^{\mathsf{s}})^{\mathsf{s}} \circ (\boldsymbol{\omega}^{\mathrm{B}}_{\mathrm{D/I}} \times \boldsymbol{\omega}^{\mathrm{B}}_{\mathrm{B/I}}) + (\boldsymbol{\omega}^{\mathrm{B}}_{\mathrm{B/I}})^{\mathsf{s}} \circ (\boldsymbol{\omega}^{\mathrm{B}}_{\mathrm{D/I}} \times (M^{\mathrm{B}} \star (\boldsymbol{\omega}^{\mathrm{B}}_{\mathrm{D/I}})^{\mathsf{s}})) + (\boldsymbol{\omega}^{\mathrm{B}}_{\mathrm{D/I}})^{\mathsf{s}} \circ (\boldsymbol{\omega}^{\mathrm{B}}_{\mathrm{B/I}} \times (M^{\mathrm{B}} \star (\boldsymbol{\omega}^{\mathrm{B}}_{\mathrm{B/I}})^{\mathsf{s}})) + (M^{\mathrm{B}} \star (\boldsymbol{\omega}^{\mathrm{B}}_{\mathrm{D/I}})^{\mathsf{s}}))^{\mathsf{s}} \circ (\boldsymbol{\omega}^{\mathrm{B}}_{\mathrm{D/I}} \times \boldsymbol{\omega}^{\mathrm{B}}_{\mathrm{B/I}})$. Finally, applying (3) and (5) to the first and last terms of the previous expression yields $-(\boldsymbol{\omega}^{\mathrm{B}}_{\mathrm{D/I}})^{\mathsf{s}} \circ (\boldsymbol{\omega}^{\mathrm{B}}_{\mathrm{B/I}} \times (M^{\mathrm{B}} \star (\boldsymbol{\omega}^{\mathrm{B}}_{\mathrm{B/I}})^{\mathsf{s}})) + (\boldsymbol{\omega}^{\mathrm{B}}_{\mathrm{B/I}})^{\mathsf{s}} \circ (\boldsymbol{\omega}^{\mathrm{B}}_{\mathrm{D/I}} \times (M^{\mathrm{B}} \star (\boldsymbol{\omega}^{\mathrm{B}}_{\mathrm{D/I}})^{\mathsf{s}})) + (\boldsymbol{\omega}^{\mathrm{B}}_{\mathrm{D/I}})^{\mathsf{s}} \circ (\boldsymbol{\omega}^{\mathrm{B}}_{\mathrm{B/I}} \times (M^{\mathrm{B}} \star (\boldsymbol{\omega}^{\mathrm{B}}_{\mathrm{B/I}})^{\mathsf{s}})) - (\boldsymbol{\omega}^{\mathrm{B}}_{\mathrm{B/I}})^{\mathsf{s}} \circ (\boldsymbol{\omega}^{\mathrm{B}}_{\mathrm{D/I}} \times (M^{\mathrm{B}} \star (\boldsymbol{\omega}^{\mathrm{B}}_{\mathrm{D/I}})^{\mathsf{s}})) = \mathbf{0}$. Therefore, the time derivative of the Lyapunov function is equal to $\dot{V} = -k_d(\boldsymbol{\omega}^{\mathrm{B}}_{\mathrm{B/D}})^{\mathsf{s}} \circ (\boldsymbol{\omega}^{\mathrm{B}}_{\mathrm{B/D}})^{\mathsf{s}} \leq 0$, for all $(\boldsymbol{q}_{\mathrm{B/D}}, \boldsymbol{\omega}^{\mathrm{B}}_{\mathrm{B/D}}) \in \mathbb{H}^u_d \times \mathbb{H}^v_d \backslash \{\mathbf{1}, \mathbf{0}\}$. Hence, $\boldsymbol{q}_{\mathrm{B/D}}$ and $\boldsymbol{\omega}^{\mathrm{B}}_{\mathrm{B/D}}$ are uniformly bounded, i.e., $\boldsymbol{q}_{\mathrm{B/D}}, \boldsymbol{\omega}^{\mathrm{B}}_{\mathrm{B/D}} \in \mathcal{L}_\infty$.

Since $V \geq 0$ and $\dot{V} \leq 0$, $\lim_{t\to\infty} V(t)$ exists and is finite. By integrating both sides of $\dot{V} = -k_d(\boldsymbol{\omega}^{\mathrm{B}}_{\mathrm{B/D}})^{\mathsf{s}} \circ (\boldsymbol{\omega}^{\mathrm{B}}_{\mathrm{B/D}})^{\mathsf{s}} \leq 0$, one obtains $\lim_{t\to\infty} \int_0^t \dot{V}(\tau)\,\mathrm{d}\tau = \lim_{t\to\infty} V(t) - V(0) \leq -\lim_{t\to\infty} \int_0^t k_d(\boldsymbol{\omega}^{\mathrm{B}}_{\mathrm{B/D}}(\tau))^{\mathsf{s}} \circ (\boldsymbol{\omega}^{\mathrm{B}}_{\mathrm{B/D}}(\tau))^{\mathsf{s}} \mathrm{d}\tau$ or

$$\lim_{t\to\infty} \int_0^t k_d(\boldsymbol{\omega}^{\mathrm{B}}_{\mathrm{B/D}}(\tau))^{\mathsf{s}} \circ (\boldsymbol{\omega}^{\mathrm{B}}_{\mathrm{B/D}}(\tau))^{\mathsf{s}}\,\mathrm{d}\tau \leq V(0). \tag{15}$$

Since $\boldsymbol{q}_{\mathrm{B/D}}, \boldsymbol{\omega}^{\mathrm{B}}_{\mathrm{B/D}} \in \mathcal{L}_\infty$ and $\dot{\boldsymbol{\omega}}^{\mathrm{D}}_{\mathrm{D/I}}, \boldsymbol{\omega}^{\mathrm{B}}_{\mathrm{D/I}} \in \mathcal{L}_\infty$ by assumption, from (14) it follows that $\boldsymbol{f}^{\mathrm{B}} \in \mathcal{L}_\infty$ as well. Then, from (13) it also follows that $\dot{\boldsymbol{\omega}}^{\mathrm{B}}_{\mathrm{B/D}} \in \mathcal{L}_\infty$. Along with (15), this implies that $\boldsymbol{\omega}^{\mathrm{B}}_{\mathrm{B/D}}(t) \to \mathbf{0}$ as $t \to \infty$, according to Barbalat's lemma [11].

It can also be shown that $\dot{\boldsymbol{\omega}}^{\mathrm{B}}_{\mathrm{B/D}} \to \mathbf{0}$ as $t \to \infty$. First, note that $\lim_{t\to\infty} \int_0^t \dot{\boldsymbol{\omega}}^{\mathrm{B}}_{\mathrm{B/D}}(\tau)\,\mathrm{d}\tau = \lim_{t\to\infty} \boldsymbol{\omega}^{\mathrm{B}}_{\mathrm{B/D}}(t) - \boldsymbol{\omega}^{\mathrm{B}}_{\mathrm{B/D}}(0) = -\boldsymbol{\omega}^{\mathrm{B}}_{\mathrm{B/D}}(0)$ exists and is finite. Now note that $\ddot{\boldsymbol{\omega}}^{\mathrm{B}}_{\mathrm{B/D}} \in \mathcal{L}_\infty$ since $\dot{\boldsymbol{\omega}}^{\mathrm{D}}_{\mathrm{D/I}}, \boldsymbol{\omega}^{\mathrm{D}}_{\mathrm{D/I}}, \dot{\boldsymbol{\omega}}^{\mathrm{B}}_{\mathrm{B/D}}, \boldsymbol{\omega}^{\mathrm{B}}_{\mathrm{B/D}}, \boldsymbol{q}_{\mathrm{B/D}}, \dot{\boldsymbol{q}}_{\mathrm{B/D}} \in \mathcal{L}_\infty$. Hence, by Barbalat's lemma, $\dot{\boldsymbol{\omega}}^{\mathrm{B}}_{\mathrm{B/D}} \to \mathbf{0}$ as $t \to \infty$.

Finally, calculating the limit as $t \to \infty$ of both sides of (13) yields $\mathrm{vec}\big(\boldsymbol{q}^*_{\mathrm{B/D}}(\boldsymbol{q}^{\mathsf{s}}_{\mathrm{B/D}} - \mathbf{1}^{\mathsf{s}})\big) \to \mathbf{0}$ as $t \to \infty$, which, as shown in [12], is equivalent to $\boldsymbol{q}_{\mathrm{B/D}} \to \pm\mathbf{1}$. ∎

Remark 1: The dual part of control law (14) is $\tau^{\mathrm{B}} = -k_p \mathrm{vec}\big(q_{\mathrm{B/D}}\big) - k_d \omega^{\mathrm{B}}_{\mathrm{B/D}} + I^{\mathrm{B}} * (q^*_{\mathrm{B/D}} \dot{\omega}^{\mathrm{D}}_{\mathrm{D/I}} q_{\mathrm{B/D}}) + \omega^{\mathrm{B}}_{\mathrm{D/I}} \times (I^{\mathrm{B}} * \omega^{\mathrm{B}}_{\mathrm{D/I}})$. This control law is identical to the attitude(-only) model-dependent control law proposed in [13].

IV. Velocity-Free Pose-Tracking Controller

The pose-tracking controller presented in Section III is almost globally asymptotically stable, but requires measurements of $\boldsymbol{\omega}^{\mathrm{B}}_{\mathrm{B/D}}$. The next theorem shows that it is still possible to obtain an almost globally asymptotically stable pose-tracking controller without measurements of $\boldsymbol{\omega}^{\mathrm{B}}_{\mathrm{B/D}}$.

Theorem 2: Consider the rigid body relative kinematic and dynamic equations (12) and (13), respectively. Let the total external dual force acting on the rigid body be defined by the feedback control law

$$\boldsymbol{f}^{\mathrm{B}} = -k_p \mathrm{vec}\big(\boldsymbol{q}^*_{\mathrm{B/D}}(\boldsymbol{q}^{\mathsf{s}}_{\mathrm{B/D}} - \mathbf{1}^{\mathsf{s}})\big) - 2\mathrm{vec}\big(\boldsymbol{q}^*_{\mathrm{B/D}} \boldsymbol{z}^{\mathsf{s}}\big) + M^{\mathrm{B}} \star (\boldsymbol{q}^*_{\mathrm{B/D}} \dot{\boldsymbol{\omega}}^{\mathrm{D}}_{\mathrm{D/I}} \boldsymbol{q}_{\mathrm{B/D}})^{\mathsf{s}} + \boldsymbol{\omega}^{\mathrm{B}}_{\mathrm{D/I}} \times (M^{\mathrm{B}} \star (\boldsymbol{\omega}^{\mathrm{B}}_{\mathrm{D/I}})^{\mathsf{s}}), \quad k_p > 0, \tag{16}$$

where $\boldsymbol{z}$ is the output of the LTI system

$$\dot{\boldsymbol{x}}_{\mathrm{p}} = A \star \boldsymbol{x}_{\mathrm{p}} + B \star \boldsymbol{q}_{\mathrm{B/D}} \text{ and } \boldsymbol{z} = (CA) \star \boldsymbol{x}_{\mathrm{p}} + (CB) \star \boldsymbol{q}_{\mathrm{B/D}}, \tag{17}$$

(A, B, C) is a minimal realization of a strictly positive real transfer matrix $C_{\mathrm{sp}}(s)$, and B a full rank matrix. Assume that $\dot{\boldsymbol{\omega}}^{\mathrm{D}}_{\mathrm{D/I}}, \boldsymbol{\omega}^{\mathrm{D}}_{\mathrm{D/I}} \in \mathcal{L}_\infty$. Then, $\boldsymbol{q}_{\mathrm{B/D}} \to \pm\mathbf{1}$, $\boldsymbol{\omega}^{\mathrm{B}}_{\mathrm{B/D}} \to \mathbf{0}$, and $\boldsymbol{x}_{\mathrm{sp}} = \dot{\boldsymbol{x}}_{\mathrm{p}} \to \mathbf{0}$ as $t \to +\infty$ for all initial conditions.

Proof: First, rewrite the LTI system as follows:

$$\dot{\boldsymbol{x}}_{\mathrm{sp}} = A \star \boldsymbol{x}_{\mathrm{sp}} + B \star \dot{\boldsymbol{q}}_{\mathrm{B/D}} \quad \text{and} \quad \boldsymbol{z} = C \star \boldsymbol{x}_{\mathrm{sp}}. \tag{18}$$

Note that $\boldsymbol{q}_{\mathrm{B/D}} = \pm\mathbf{1}$, $\boldsymbol{\omega}^{\mathrm{B}}_{\mathrm{B/D}} = \mathbf{0}$, and $\boldsymbol{x}_{\mathrm{sp}} = \mathbf{0}$ is the equilibrium condition of the closed-loop system formed by (13), (12), (18), and (16). Consider the candidate Lyapunov function $V(\boldsymbol{q}_{\mathrm{B/D}}, \boldsymbol{\omega}^{\mathrm{B}}_{\mathrm{B/D}}, \boldsymbol{x}_{\mathrm{sp}}) = k_p(\boldsymbol{q}_{\mathrm{B/D}} - \mathbf{1}) \circ (\boldsymbol{q}_{\mathrm{B/D}} - \mathbf{1}) + \frac{1}{2}(\boldsymbol{\omega}^{\mathrm{B}}_{\mathrm{B/D}})^{\mathsf{s}} \circ (M^{\mathrm{B}} \star (\boldsymbol{\omega}^{\mathrm{B}}_{\mathrm{B/D}})^{\mathsf{s}}) + 2\boldsymbol{x}_{\mathrm{sp}} \circ (P \star \boldsymbol{x}_{\mathrm{sp}})$, for the equilibrium point $\boldsymbol{q}_{\mathrm{B/D}} = \mathbf{1}$, $\boldsymbol{\omega}^{\mathrm{B}}_{\mathrm{B/D}} = \mathbf{0}$, and $\boldsymbol{x}_{\mathrm{sp}} = \mathbf{0}$, where $P = P^{\mathsf{T}} > 0$ satisfies $A^{\mathsf{T}}P + PA = -Q$, $PB = C^{\mathsf{T}}$, and $Q = Q^{\mathsf{T}} > 0$. By the Kalman-Yakubovich-Popov (KYP) conditions [11], there always exist matrices P and Q satisfying these conditions, since (A, B, C) is a minimal realization of a strictly positive real transfer matrix $C_{\mathrm{sp}}(s)$. Note that V is a valid candidate Lyapunov function since $V(\boldsymbol{q}_{\mathrm{B/D}} = \mathbf{1}, \boldsymbol{\omega}^{\mathrm{B}}_{\mathrm{B/D}} = \mathbf{0}, \boldsymbol{x}_{\mathrm{sp}} = \mathbf{0}) = 0$ and $V(\boldsymbol{q}_{\mathrm{B/D}}, \boldsymbol{\omega}^{\mathrm{B}}_{\mathrm{B/D}}, \boldsymbol{x}_{\mathrm{sp}}) > 0$ for all $(\boldsymbol{q}_{\mathrm{B/D}}, \boldsymbol{\omega}^{\mathrm{B}}_{\mathrm{B/D}}, \boldsymbol{x}_{\mathrm{sp}}) \in \mathbb{H}^u_d \times$

$\mathbb{H}_d^v \times \mathbb{H}_d \backslash \{\mathbf{1}, \mathbf{0}, \mathbf{0}\}$. The time derivative of V is equal to $\dot{V} = 2k_p(\boldsymbol{q}_{\text{B/D}} - \mathbf{1}) \circ \dot{\boldsymbol{q}}_{\text{B/D}} + (\boldsymbol{\omega}^{\text{B}}_{\text{B/D}})^{\text{S}} \circ (M^{\text{B}} \star (\dot{\boldsymbol{\omega}}^{\text{B}}_{\text{B/D}})^{\text{S}}) + 4\dot{\boldsymbol{x}}_{\text{sp}} \circ (P \star \boldsymbol{x}_{\text{sp}})$. By plugging in (12) and (13) and applying (2) and the KYP conditions, it follows that $\dot{V} = (\boldsymbol{\omega}^{\text{B}}_{\text{B/D}})^{\text{S}} \circ (k_p \boldsymbol{q}^*_{\text{B/D}} (\boldsymbol{q}^{\text{S}}_{\text{B/D}} - \mathbf{1}^{\text{S}}) + \boldsymbol{f}^{\text{B}} - (\boldsymbol{\omega}^{\text{B}}_{\text{B/D}} + \boldsymbol{\omega}^{\text{B}}_{\text{D/I}}) \times (M^{\text{B}} \star ((\boldsymbol{\omega}^{\text{B}}_{\text{B/D}})^{\text{S}} + (\boldsymbol{\omega}^{\text{B}}_{\text{D/I}}))^{\text{S}}) - M^{\text{B}} \star (\boldsymbol{q}^*_{\text{B/D}} \dot{\boldsymbol{\omega}}^{\text{D}}_{\text{D/I}} \boldsymbol{q}_{\text{B/D}})^{\text{S}} - M^{\text{B}} \star (\boldsymbol{\omega}^{\text{B}}_{\text{D/I}} \times \boldsymbol{\omega}^{\text{B}}_{\text{B/D}})^{\text{S}}) + 4(A \star \boldsymbol{x}_{\text{sp}} + B \star \dot{\boldsymbol{q}}_{\text{B/D}}) \circ (P \star \boldsymbol{x}_{\text{sp}})$. Introducing the feedback control law (16) yields $\dot{V} = (\boldsymbol{\omega}^{\text{B}}_{\text{B/D}})^{\text{S}} \circ (-2\text{vec}(\boldsymbol{q}^*_{\text{B/D}} \boldsymbol{z}^{\text{S}})) + (\boldsymbol{\omega}^{\text{B}}_{\text{B/D}})^{\text{S}} \circ (k_p \boldsymbol{q}^*_{\text{B/D}} (\boldsymbol{q}^{\text{S}}_{\text{B/D}} - \mathbf{1}^{\text{S}}) - k_p \text{vec}(\boldsymbol{q}^*_{\text{B/D}} (\boldsymbol{q}^{\text{S}}_{\text{B/D}} - \mathbf{1}^{\text{S}}))) + (\boldsymbol{\omega}^{\text{B}}_{\text{B/D}})^{\text{S}} \circ (-(\boldsymbol{\omega}^{\text{B}}_{\text{B/D}} + \boldsymbol{\omega}^{\text{B}}_{\text{D/I}}) \times (M^{\text{B}} \star ((\boldsymbol{\omega}^{\text{B}}_{\text{B/D}})^{\text{S}} + (\boldsymbol{\omega}^{\text{B}}_{\text{D/I}}))^{\text{S}}) - M^{\text{B}} \star (\boldsymbol{\omega}^{\text{B}}_{\text{D/I}} \times \boldsymbol{\omega}^{\text{B}}_{\text{B/D}})^{\text{S}} + \boldsymbol{\omega}^{\text{B}}_{\text{D/I}} \times (M^{\text{B}} \star (\boldsymbol{\omega}^{\text{B}}_{\text{D/I}})^{\text{S}})) + 4(A \star \boldsymbol{x}_{\text{sp}} + B \star \dot{\boldsymbol{q}}_{\text{B/D}}) \circ (P \star \boldsymbol{x}_{\text{sp}})$. Again, note that the second term is zero because it is the circle product of a dual vector quaternion with a dual scalar quaternion. Moreover, the third term has been shown to be equal to zero in the proof of Theorem 1. As for the fourth term, it can be simplified as follows: $\dot{V} = (\boldsymbol{\omega}^{\text{B}}_{\text{B/D}})^{\text{S}} \circ (-2\text{vec}(\boldsymbol{q}^*_{\text{B/D}} \boldsymbol{z}^{\text{S}})) + 4(A \star \boldsymbol{x}_{\text{sp}}) \circ (P \star \boldsymbol{x}_{\text{sp}}) + 4(B \star \dot{\boldsymbol{q}}_{\text{B/D}}) \circ (P \star \boldsymbol{x}_{\text{sp}}) = (\boldsymbol{\omega}^{\text{B}}_{\text{B/D}})^{\text{S}} \circ (-2\text{vec}(\boldsymbol{q}^*_{\text{B/D}} \boldsymbol{z}^{\text{S}})) + 2((A^{\text{T}}P + PA) \star \boldsymbol{x}_{\text{sp}}) \circ \boldsymbol{x}_{\text{sp}} + 4\dot{\boldsymbol{q}}_{\text{B/D}} \circ ((B^T P) \star \boldsymbol{x}_{\text{sp}}) = (\boldsymbol{\omega}^{\text{B}}_{\text{B/D}})^{\text{S}} \circ (-2\text{vec}(\boldsymbol{q}^*_{\text{B/D}} \boldsymbol{z}^{\text{S}})) - 2\boldsymbol{x}_{\text{sp}} \circ (Q \star \boldsymbol{x}_{\text{sp}}) + 2(\boldsymbol{q}_{\text{B/D}} \boldsymbol{\omega}^{\text{B}}_{\text{B/D}}) \circ (C \star \boldsymbol{x}_{\text{sp}}) = (\boldsymbol{\omega}^{\text{B}}_{\text{B/D}})^{\text{S}} \circ (2\boldsymbol{q}^*_{\text{B/D}} \boldsymbol{z}^{\text{S}} - 2\text{vec}(\boldsymbol{q}^*_{\text{B/D}} \boldsymbol{z}^{\text{S}})) - 2\boldsymbol{x}_{\text{sp}} \circ (Q \star \boldsymbol{x}_{\text{sp}}) = -2\boldsymbol{x}_{\text{sp}} \circ (Q \star \boldsymbol{x}_{\text{sp}}) \leq 0$, for all $(\boldsymbol{q}_{\text{B/D}}, \boldsymbol{\omega}^{\text{B}}_{\text{B/D}}, \boldsymbol{x}_{\text{sp}}) \in \mathbb{H}_d^u \times \mathbb{H}_d^v \times \mathbb{H}_d \backslash \{\mathbf{1}, \mathbf{0}, \mathbf{0}\}$. Hence, $\boldsymbol{q}_{\text{B/D}}$, $\boldsymbol{\omega}^{\text{B}}_{\text{B/D}}$, and $\boldsymbol{x}_{\text{sp}}$ are uniformly bounded, i.e., $\boldsymbol{q}_{\text{B/D}}, \boldsymbol{\omega}^{\text{B}}_{\text{B/D}}, \boldsymbol{x}_{\text{sp}} \in \mathcal{L}_\infty$.

It is now shown that $\boldsymbol{x}_{\text{sp}} \to \mathbf{0}$ as $t \to \infty$. Since $V \geq 0$ and $\dot{V} \leq 0$, $\lim_{t\to\infty} V(t)$ exists and is finite. By integrating both sides of $\dot{V} = -2\boldsymbol{x}_{\text{sp}} \circ (Q \star \boldsymbol{x}_{\text{sp}}) \leq 0$, one obtains $\lim_{t\to\infty} \int_0^t \dot{V}(\tau)\,\mathrm{d}\tau = \lim_{t\to\infty} V(t) - V(0) = -\lim_{t\to\infty} \int_0^t 2\boldsymbol{x}_{\text{sp}}(\tau) \circ (Q \star \boldsymbol{x}_{\text{sp}}(\tau))\mathrm{d}\tau$ or

$$\lim_{t\to\infty} \int_0^t 2\boldsymbol{x}_{\text{sp}}(\tau) \circ (Q \star \boldsymbol{x}_{\text{sp}}(\tau))\,\mathrm{d}\tau \leq V(0). \tag{19}$$

Since $\boldsymbol{q}_{\text{B/D}}, \boldsymbol{\omega}^{\text{B}}_{\text{B/D}}, \boldsymbol{x}_{\text{sp}} \in \mathcal{L}_\infty$, it follows that $\dot{\boldsymbol{q}}_{\text{B/D}} \in \mathcal{L}_\infty$ and $\dot{\boldsymbol{x}}_{\text{sp}} \in \mathcal{L}_\infty$. Along with (19), this implies that $\boldsymbol{x}_{\text{sp}} \to \mathbf{0}$ as $t \to \infty$, according to Barbalat's lemma. This, in turn, implies that $\boldsymbol{z} \to \mathbf{0}$ as $t \to \infty$ from (18).

It can also be shown that $\dot{\boldsymbol{x}}_{\text{sp}} \to \mathbf{0}$ as $t \to \infty$. First, note that $\lim_{t\to\infty} \int_0^t \dot{\boldsymbol{x}}_{\text{sp}}(\tau)\,\mathrm{d}\tau = \lim_{t\to\infty} \boldsymbol{x}_{\text{sp}}(t) - \boldsymbol{x}_{\text{sp}}(0) = -\boldsymbol{x}_{\text{sp}}(0)$ exists and is finite. Since $\ddot{\boldsymbol{x}}_{\text{sp}} = A \star \dot{\boldsymbol{x}}_{\text{sp}} + B \star \ddot{\boldsymbol{q}}_{\text{B/D}}$ and

$$\boldsymbol{q}_{\text{B/D}}, \boldsymbol{\omega}^{\text{B}}_{\text{B/D}}, \boldsymbol{x}_{\text{sp}}, \dot{\boldsymbol{q}}_{\text{B/D}}, \dot{\boldsymbol{x}}_{\text{sp}}, \dot{\boldsymbol{\omega}}^{\text{D}}_{\text{D/I}}, \boldsymbol{\omega}^{\text{D}}_{\text{D/I}}, \boldsymbol{z}, \dot{\boldsymbol{\omega}}^{\text{B}}_{\text{B/D}}, \ddot{\boldsymbol{q}}_{\text{B/D}} \in \mathcal{L}_\infty,$$

it follows that $\ddot{\boldsymbol{x}}_{\text{sp}} \in \mathcal{L}_\infty$. Hence, by Barbalat's lemma, $\dot{\boldsymbol{x}}_{\text{sp}} \to \mathbf{0}$ as $t \to \infty$.

Thus, calculating the limit as $t \to \infty$ of both sides of (18) yields $\dot{\boldsymbol{q}}_{\text{B/D}} \to \mathbf{0}$ as $t \to \infty$, since B is assumed to be full rank. Given that (12) can be rewritten as $\boldsymbol{\omega}^{\text{B}}_{\text{B/D}} = 2\boldsymbol{q}^*_{\text{B/D}} \dot{\boldsymbol{q}}_{\text{B/D}}$, this also implies that $\boldsymbol{\omega}^{\text{B}}_{\text{B/D}} \to \mathbf{0}$ as $t \to \infty$.

Now, it is shown that $\dot{\boldsymbol{\omega}}^{\text{B}}_{\text{B/D}} \to \mathbf{0}$ as $t \to \infty$. First, note that $\lim_{t\to\infty} \int_0^t \dot{\boldsymbol{\omega}}^{\text{B}}_{\text{B/D}}(\tau)\,\mathrm{d}\tau = \lim_{t\to\infty} \boldsymbol{\omega}^{\text{B}}_{\text{B/D}}(t) - \boldsymbol{\omega}^{\text{B}}_{\text{B/D}}(0) = -\boldsymbol{\omega}^{\text{B}}_{\text{B/D}}(0)$ exists and is finite. Since $(\ddot{\boldsymbol{\omega}}^{\text{B}}_{\text{B/D}})^{\text{S}} = (M^{\text{B}})^{-1} \star (-k_p \text{vec}(\dot{\boldsymbol{q}}^*_{\text{B/D}} (\boldsymbol{q}^{\text{S}}_{\text{B/D}} - \mathbf{1}^{\text{S}})) - k_p \text{vec}(\boldsymbol{q}^*_{\text{B/D}} (\dot{\boldsymbol{q}}^{\text{S}}_{\text{B/D}})) - 2\text{vec}(\dot{\boldsymbol{q}}^*_{\text{B/D}} \boldsymbol{z}^{\text{S}}) - 2\text{vec}(\boldsymbol{q}^*_{\text{B/D}} (\dot{\boldsymbol{z}})^{\text{S}}) + \dot{\boldsymbol{\omega}}^{\text{B}}_{\text{D/I}} \times (M^{\text{B}} \star (\boldsymbol{\omega}^{\text{B}}_{\text{D/I}})^{\text{S}}) + \boldsymbol{\omega}^{\text{B}}_{\text{D/I}} \times (M^{\text{B}} \star (\dot{\boldsymbol{\omega}}^{\text{B}}_{\text{D/I}})^{\text{S}}) - \dot{\boldsymbol{\omega}}^{\text{B}}_{\text{B/I}} \times (M^{\text{B}} \star (\boldsymbol{\omega}^{\text{B}}_{\text{B/I}})^{\text{S}}) - \boldsymbol{\omega}^{\text{B}}_{\text{B/I}} \times (M^{\text{B}} \star (\dot{\boldsymbol{\omega}}^{\text{B}}_{\text{B/I}})^{\text{S}}) - M^{\text{B}} \star (\dot{\boldsymbol{\omega}}^{\text{B}}_{\text{D/I}} \times \boldsymbol{\omega}^{\text{B}}_{\text{B/D}})^{\text{S}} - M^{\text{B}} \star (\boldsymbol{\omega}^{\text{B}}_{\text{D/I}} \times \dot{\boldsymbol{\omega}}^{\text{B}}_{\text{B/D}})^{\text{S}})$ and $\dot{\boldsymbol{\omega}}^{\text{B}}_{\text{B/D}}, \boldsymbol{\omega}^{\text{B}}_{\text{B/D}}, \dot{\boldsymbol{\omega}}^{\text{B}}_{\text{B/I}}, \boldsymbol{\omega}^{\text{B}}_{\text{B/I}}, \boldsymbol{q}_{\text{B/D}}, \dot{\boldsymbol{q}}_{\text{B/D}}, \boldsymbol{z}, \dot{\boldsymbol{z}} \in \mathcal{L}_\infty$, it follows that $\ddot{\boldsymbol{\omega}}^{\text{B}}_{\text{B/D}} \in \mathcal{L}_\infty$. Hence, by Barbalat's lemma, $\dot{\boldsymbol{\omega}}^{\text{B}}_{\text{B/D}} \to \mathbf{0}$ as $t \to \infty$.

Finally, calculating the limit as $t \to \infty$ of both sides of (13) yields $\text{vec}(\boldsymbol{q}^*_{\text{B/D}} (\boldsymbol{q}^{\text{S}}_{\text{B/D}} - \mathbf{1}^{\text{S}})) \to \mathbf{0}$ as $t \to \infty$, which, as shown in [12], is equivalent to $\boldsymbol{q}_{\text{B/D}} \to \pm\mathbf{1}$. ■

Remark 2: Theorems 1 and 2 state that $\boldsymbol{q}_{\text{B/D}}$ converges to either $+\mathbf{1}$ or $-\mathbf{1}$. Note that $\boldsymbol{q}_{\text{B/D}} = +\mathbf{1}$ and $\boldsymbol{q}_{\text{B/D}} = -\mathbf{1}$ represent the same pose [10]. Therefore, either equilibrium is acceptable. However, this can lead to the so-called *unwinding phenomenon*, where a large rotation (greater than 180 deg) is performed despite the fact that a smaller rotation (less than 180 deg) exists. This problem of quaternions is well documented and possible solutions exist in literature [7].

Remark 3: If the reference pose is constant, i.e., $\boldsymbol{\omega}^{\text{D}}_{\text{D/I}} = \mathbf{0}$, then the pose-tracking controllers suggested in Theorems 1 and 2 become pose-stabilization controllers [12]. Note that in this special case, the feedback control laws (14) and (16) do not depend on M^{B}, i.e., they do not depend on the mass and inertia matrix of the rigid body.

Remark 4: By choosing A and B as $-k_f I_{8\times 8}$ and $k_f I_{8\times 8}$ in (17), respectively, where $k_f > 0$, and by defining $Q = -k_d(B^{-\text{T}} A + A^{\text{T}} B^{-\text{T}})$ as in [14], the KYP conditions yield $P = k_d B^{-\text{T}}$ and $C = k_d I_{8\times 8}$. Then, the transfer matrix representation of the LTI system (17) is given by $C_{\text{p}}(s) = ds/(s+a)$, where $d = k_d k_f$ and $a = k_f$. In this case, $\boldsymbol{z}$ is obtained by differentiating $\boldsymbol{q}_{\text{B/D}}$ and passing $\dot{\boldsymbol{q}}_{\text{B/D}}$ through a low-pass filter. Theorem 2 proves that in the absence of measurement noise, the cut-off frequency of the low-pass filter can be chosen arbitrarily. In practice, in the presence of measurement noise, the cut-off frequency of the low-pass filter has to be chosen low enough to reject high-frequency measurement noise.

V. Simulation Results

The velocity-feedback and the velocity-free pose-tracking controllers given by (14) and (16) are numerically verified and compared in this section via two examples. In the first example, a chaser spacecraft is required to track an elliptical motion around a target satellite while pointing at it. In the second example, the velocity-free controller is compared qualitatively and quantitatively to the velocity-feedback controller fed with velocity estimates produced by an EKF through a more realistic satellite proximity operations simulation.

A. Satellite Proximity Operations Example

The first example consists of a satellite proximity operations scenario where a chaser satellite is required to track an elliptical motion around a target satellite while pointing at it.

Four reference frames are defined: the inertial frame, the target frame, the desired frame, and the body frame. The inertial frame is the Earth-Centered-Inertial (ECI) frame. The body frame is some frame fixed to the chaser satellite and centered at its center of mass. The target frame is defined as $\bar{I}_{\text{T}} = \bar{r}_{\text{T/I}}/\|\bar{r}_{\text{T/I}}\|$, $\bar{J}_{\text{T}} = \bar{K}_{\text{T}} \times \bar{I}_{\text{T}}$, and $\bar{K}_{\text{T}} = \bar{\omega}_{\text{T/I}}/\|\bar{\omega}_{\text{T/I}}\|$. The desired frame are defined as $\bar{I}_{\text{D}} = \bar{r}_{\text{D/T}}/\|\bar{r}_{\text{D/T}}\|$, $\bar{J}_{\text{D}} = \bar{K}_{\text{D}} \times \bar{I}_{\text{D}}$, and $\bar{K}_{\text{D}} = \bar{\omega}_{\text{D/T}}/\|\bar{\omega}_{\text{D/T}}\|$ [7]. The target satellite is assumed to be fixed to the target frame. The different frames are illustrated in Fig. 1. The control objective is to superimpose the body frame onto the desired frame.

The target spacecraft is assumed to be in a highly eccentric Molniya orbit with initial orbital elements given in [7] and nadir pointing. The relative motion of the desired frame with

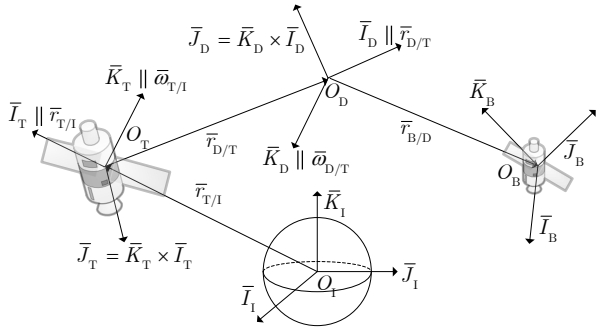

Fig. 1. Reference frames.

respect to the target frame is defined as an ellipse in the $\bar{I}_{\rm T}$-$\bar{J}_{\rm T}$ plane with semi-major axis equal to 20 m along $\bar{J}_{\rm T}$ and semi-minor axis equal to 10 m along $\bar{I}_{\rm T}$. The relative orbit has constant angular speed equal to the mean motion of the target satellite. More precisely, during this phase, $\bar{\omega}^{\rm T}_{\rm D/T} = [0\ 0\ n]^{\rm T}$ rad/s, $\bar{v}^{\rm T}_{\rm D/T} = [-a_e n \sin(nt)\ b_e n \cos(nt)\ 0]^{\rm T}$ m/s, and $\bar{r}^{\rm T}_{\rm D/T}(0)$=$[a_e\ 0\ 0]^{\rm T}$ m, where $a_e = 10$ m, $b_e = 20$ m, $n = \sqrt{\mu/a^3}$ is the (unperturbed) mean motion of the target satellite, and a is the (unperturbed) semi-major axis of the target satellite.

The linear velocity of the target satellite with respect to the inertial frame is calculated by numerically integrating the gravitational acceleration [10, eq. (73)] and also the perturbing acceleration due to Earth's oblateness [10, eq. (75)]. See [7] for expressions for the angular acceleration of the target satellite with respect to the inertial frame expressed in the inertial frame, $\alpha^{\rm I}_{\rm T/I}$, and for expressions for the variables $\boldsymbol{\omega}^{\rm D}_{\rm D/I}$ and $\dot{\boldsymbol{\omega}}^{\rm D}_{\rm D/I}$.

In this example, the total external dual force acting on the chaser spacecraft is decomposed as $\boldsymbol{f}^{\rm B} = \boldsymbol{f}^{\rm B}_g + \boldsymbol{f}^{\rm B}_{\nabla g} + \boldsymbol{f}^{\rm B}_{J_2} + \boldsymbol{f}^{\rm B}_c$, where $\boldsymbol{f}^{\rm B}_g$ is the gravitational force [10, eq. (73)], $\boldsymbol{f}^{\rm B}_{\nabla g}$ is the gravity gradient torque [10, eq. (74)], $\boldsymbol{f}^{\rm B}_{J_2}$ is the perturbing force due to Earth's oblateness [10, eq. (75)], and $\boldsymbol{f}^{\rm B}_c$ is the dual control force. In turn, the dual control force is calculated as $\boldsymbol{f}^{\rm B}_c = \boldsymbol{f}^{\rm B} - \boldsymbol{f}^{\rm B}_g - \boldsymbol{f}^{\rm B}_{\nabla g} - \boldsymbol{f}^{\rm B}_{J_2}$, where $\boldsymbol{f}^{\rm B}$ is given by either (14) or (16).

The mass and inertia matrix of the chaser satellite are assumed to be $m = 100$ kg and

$$\bar{I}^{\rm B} = \begin{bmatrix} 22 & 0.2 & 0.5 \\ 0.2 & 20 & 0.4 \\ 0.5 & 0.4 & 23 \end{bmatrix} \ \text{kg} \cdot \text{m}^2.$$

The initial conditions for this example are $\bar{r}^{\rm B}_{\rm B/D}(0)$=$[5\ 5\ 5]^{\rm T}$ m, $q_{\rm B/D}(0) = (0.3320, [0.4618\ 0.1917\ 0.7999]^{\rm T})$, $\bar{v}^{\rm B}_{\rm B/D}(0) = [0.1\ 0.1\ 0.1]^{\rm T}$ m/s, $\bar{\omega}^{\rm B}_{\rm B/D}(0) = [0.1\ 0.1\ 0.1]^{\rm T}$ rad/s, and $\boldsymbol{x}_{\rm P}(0) = \boldsymbol{q}_{\rm B/D}(0)$.

The control gains are chosen as $k_p = 0.2$, in (14) and (16), and $k_d = 4$, in (14). The matrices of the LTI system are chosen as in Remark 4 with $k_f = 10$.

Fig. 2 shows the linear and angular velocity of the desired frame with respect to the inertial frame expressed in the desired frame for the complete maneuver. These signals represent the desired motion.

Fig. 3 shows the initial transient response of the pose of the body frame with respect to the desired frame obtained

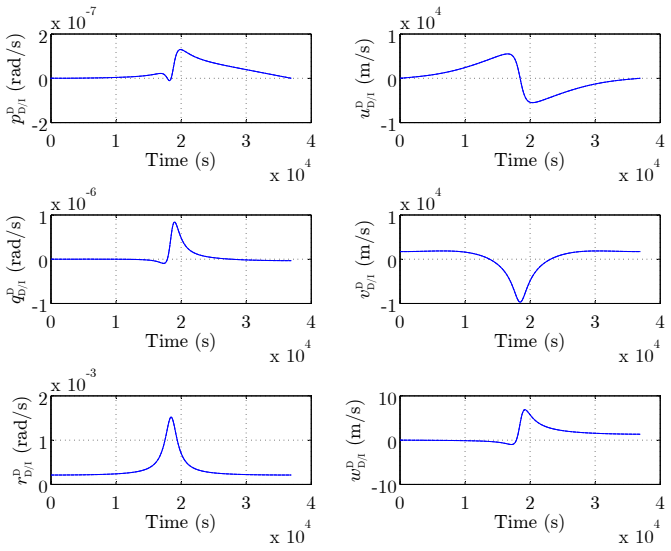

Fig. 2. Reference motion.

with (14) (control law with velocity feedback) and with (16) (control law without velocity feedback). Both controllers are able to superimpose the body frame onto the desired frame after the initial transient response.

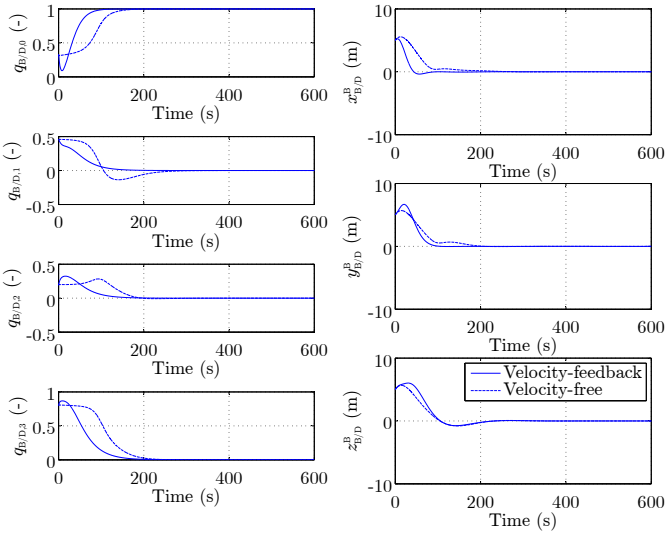

Fig. 3. Pose of the body frame with respect to the desired frame.

Fig. 4 shows the linear and angular velocity of the body frame with respect to the desired frame obtained with (14) and (16). Again, after the initial transient response, both controllers cancel the relative linear and angular velocity of the body frame with respect to the desired frame.

Fig. 5 shows the control force and control torque during the initial transient response produced by (14) and (16). For completeness, Fig. 6 shows the control force and torque for the complete maneuver. As a comparison, the complete maneuver requires a ΔV of 0.6303 m/s if done with (14) (with velocity feedback) and 0.0211 m/s more if done with (16) (without velocity feedback).

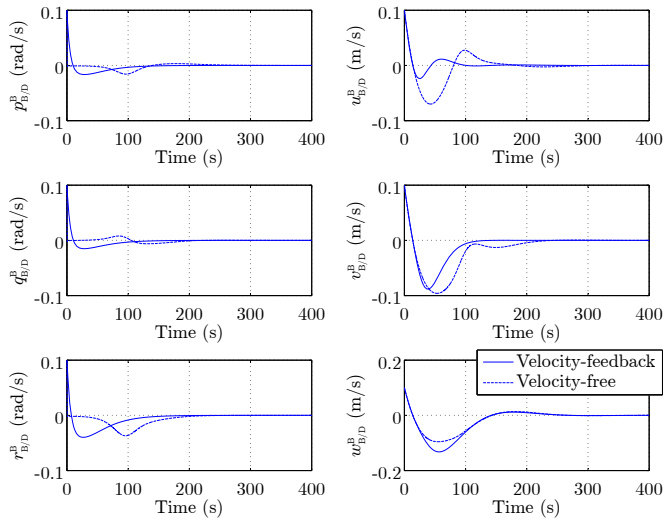

Fig. 4. Velocities of the body frame with respect to the desired frame.

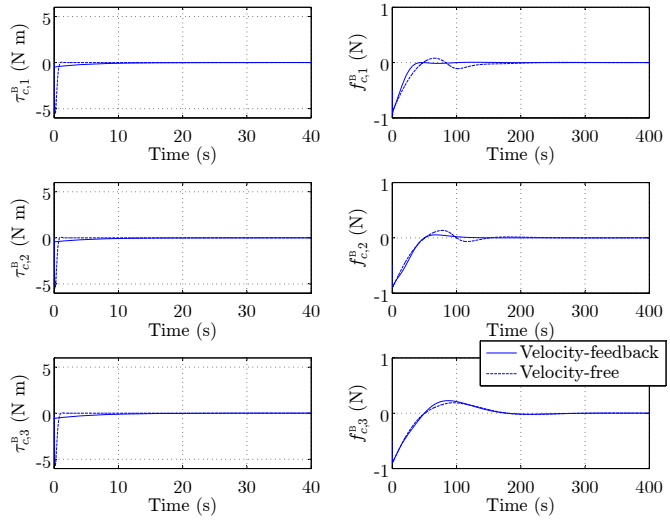

Fig. 5. Control force and torque during the initial transient response.

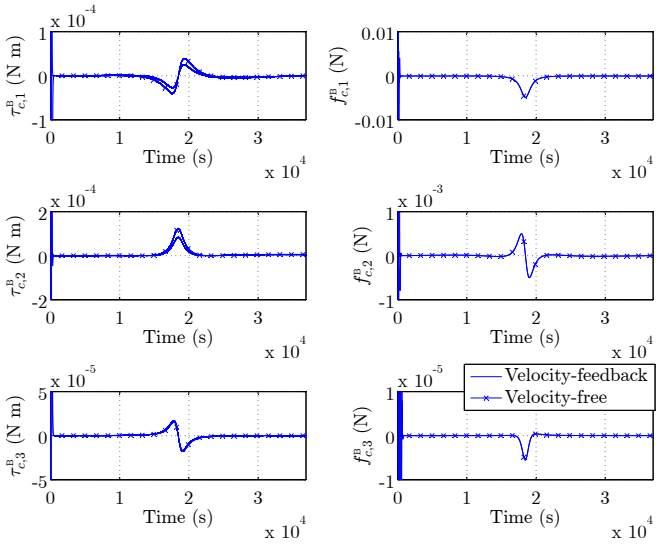

Fig. 6. Control force and torque during the complete maneuver.

B. Comparison between the Velocity-Free Controller and the Velocity-Feedback Controller with EKF

Instead of using the velocity-free pose-tracking controller derived in Theorem 2 when measurements of $\boldsymbol{\omega}^{\mathrm{B}}_{\mathrm{B/D}}$ are not available, one could use the velocity-feedback pose-tracking controller derived in Theorem 1 and an Extended Kalman Filter (EKF) to estimate the unmeasured $\boldsymbol{\omega}^{\mathrm{B}}_{\mathrm{B/D}}$ from measurements of $\boldsymbol{q}_{\mathrm{B/D}}$. The theoretical and numerical advantages and disadvantages of each solution are analyzed in this section.

The first solution has three main advantages over the second solution. The first main advantage is that under the conditions specified in Theorem 2, pose-tracking is guaranteed (i.e., $\boldsymbol{q}_{\mathrm{B/D}} \to \pm\mathbf{1}$ and $\boldsymbol{\omega}^{\mathrm{B}}_{\mathrm{B/D}} \to \mathbf{0}$ as $t \to +\infty$) independently of the initial condition chosen for $\boldsymbol{x}_{\mathrm{p}}$. On the other hand, because an EKF is based on first-order approximations, if the initial guess of the state is not close enough to the true state, the EKF may diverge, causing the velocity-feedback controller to fail. The second main advantage of the velocity-free controller is that, according to Theorem 2, the LTI system in the feedback-loop can be designed independently of the value of k_p, without violation of the almost globally asymptotically stability of the closed-loop system. On the other hand, there is no theoretical guarantee that the connection between the velocity-feedback controller derived in Theorem 1 and an EKF will ensure pose-tracking. The third and final main advantage of the velocity-free controller is the fewer number of states. For example, whereas the velocity-free controller requires the propagation of 8 states, the Dual Quaternion Multiplicative EKF (DQ-MEKF) to estimate $\boldsymbol{\omega}^{\mathrm{B}}_{\mathrm{B/D}}$ from measurements of $\boldsymbol{q}_{\mathrm{B/D}}$ described in [8] requires the propagation of 92 states (mostly due to the propagation of the state covariance matrix). This might make the velocity-free controller more suitable for satellites with limited computational resources.

On the other hand, the solution based on the velocity-feedback controller and an EKF has three important advantages over the velocity-free controller. First, an EKF can handle measurement noise by design, whereas the model on which the velocity-free controller is based assumes no noise. Note however that, for example, by choosing the matrices of the LTI system as in Remark 4, the user is free to choose the cutoff frequency of the low-pass filter in the feedback loop, which will help filter out measurement noise. Second, an EKF can be easily designed to handle discrete-time measurements, whereas the velocity-free controller described in Theorem 2 assumes continuous-time measurements. Finally, an EKF can produce a direct estimate of $\boldsymbol{\omega}^{\mathrm{B}}_{\mathrm{B/D}}$, whereas the velocity-free controller cannot. This estimate can be used to estimate $\boldsymbol{\omega}^{\mathrm{B}}_{\mathrm{D/I}} = \boldsymbol{\omega}^{\mathrm{B}}_{\mathrm{B/I}} - \boldsymbol{\omega}^{\mathrm{B}}_{\mathrm{B/D}}$, which in turn is used in both (14) and (16). In an uncooperative satellite proximity operations scenario, where $\boldsymbol{\omega}^{\mathrm{B}}_{\mathrm{D/I}}$ is unknown, and assuming that the chaser satellite can measure its own linear and angular velocities with respect to the inertial frame, i.e., $\boldsymbol{\omega}^{\mathrm{B}}_{\mathrm{B/I}}$, this provides a method to estimate $\boldsymbol{\omega}^{\mathrm{B}}_{\mathrm{D/I}}$, which is not available with the velocity-free controller. Most important, the EKF provides a measure of the uncertainty associated with the estimate of $\boldsymbol{\omega}^{\mathrm{B}}_{\mathrm{B/D}}$ through the state covariance matrix.

To compare the two solutions numerically, both controllers were applied to the satellite proximity operations scenario described in Section V-A, but now under more realistic conditions. Instead of continuous-time measurements, both controllers were now fed pose measurements at 10 Hz. Since the velocity-free controller requires continuous-time measurements, a Zero-Order-Hold (ZOH) was used to convert the discrete-time measurements into continuous-time signals. The EKF used in this comparison is the DQ-MEKF described in [8] that estimates $\boldsymbol{\omega}^{\mathrm{B}}_{\mathrm{B/D}}$ from discrete-time measurements of the relative pose. Moreover, zero-mean Additive White Gaussian Noise (AWGN) is added to the measurements of $q_{\mathrm{B/D}}$ and $r^{\mathrm{B}}_{\mathrm{B/D}}$, with standard deviation of 1×10^{-4} (-) and 1.7×10^{-3} m, respectively. After the AWGN is added to $q_{\mathrm{B/D}}$, $q_{\mathrm{B/D}}$ is re-normalized through $q_{\mathrm{B/D}} = (1/\|q_{\mathrm{B/D}}\|)q_{\mathrm{B/D}}$ [15]. Additionally, each element of the control torque and force is saturated at ± 5 N$\cdot$m and ± 5 N, respectively. Also, the controllers are run at 100 Hz to simulate a satellite with limited computational resources. Finally, to make the comparison fair, the controls gains are chosen as $k_p = 0.2$ and $k_d = 0.4$ both in (14) and in (16). All other parameters of the scenario are defined as in Section V-A.

Fig. 7 shows the initial transient response of the true (i.e., continuous-time and noise-free) pose of the body frame with respect to the desired frame obtained with the velocity-free controller and with the velocity-feedback controller in series with the DQ-MEKF. It demonstrates that, even under these more realistic conditions, both controllers can track the desired pose. In fact, Fig. 7 is relatively similar to Fig. 3, obtained under ideal conditions. The pose-tracking error is shown in more detail in Fig. 8. Whereas the pose-tracking error during the transient response is smaller with the velocity-feedback controller and the DQ-MEKF, both controllers achieve similar steady-state errors.

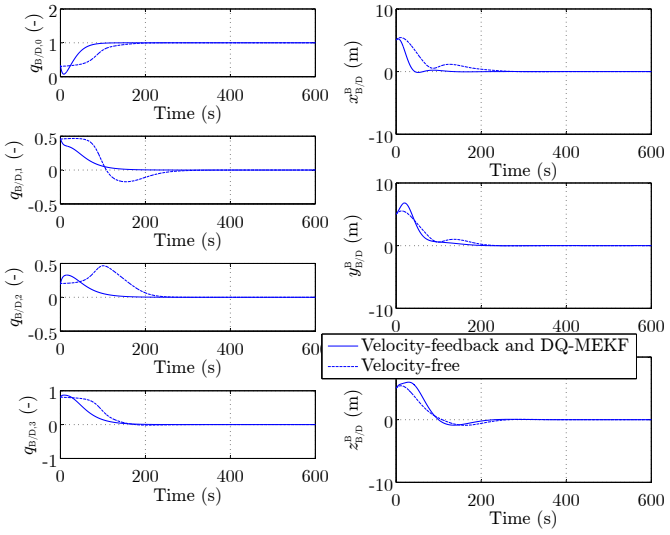

Fig. 7. Pose-tracking using the velocity-free controller and the velocity-feedback controller with the DQ-MEKF.

Fig. 9 shows the true (i.e., continuous-time and noise-free) linear and angular velocity of the body frame with respect to the desired frame obtained with both solutions under these more realistic conditions. Both controllers track the desired velocities. Again, note that Fig. 9 is relatively similar to Fig. 4, obtained under ideal conditions.

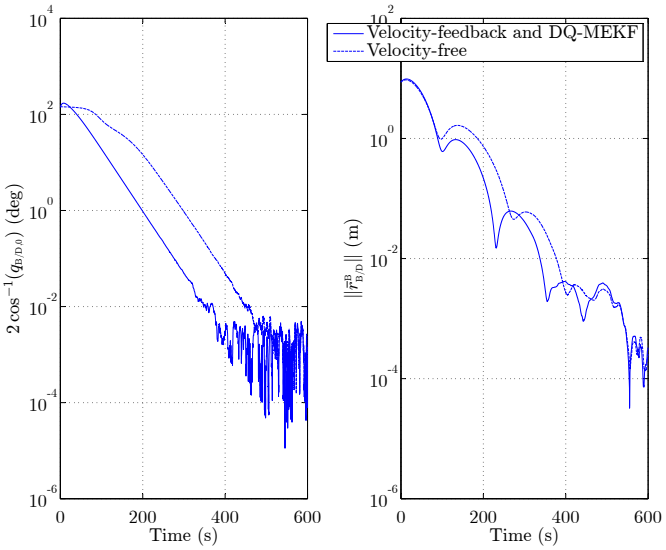

Fig. 8. Pose-tracking error using the velocity-free controller and the velocity-feedback controller with the DQ-MEKF.

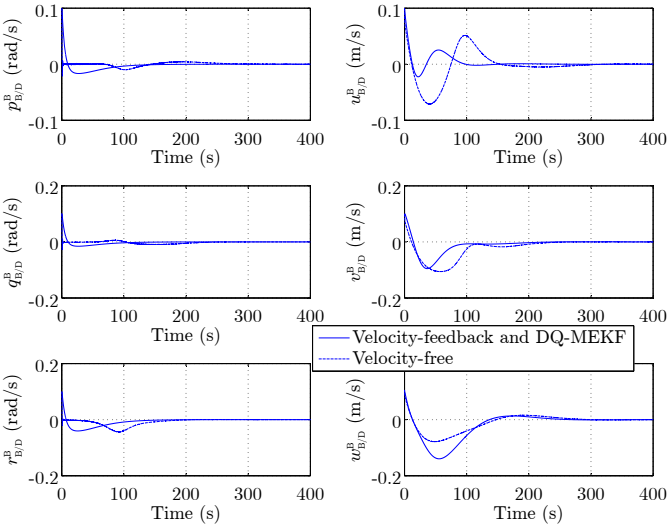

Fig. 9. Relative linear and angular velocity using the velocity-free controller and the velocity-feedback controller with the DQ-MEKF.

Finally, Fig. 10 shows the control force and torque produced by both controllers under these more realistic conditions. The control force and torque produced by the velocity-free controller exhibits noise and oscillations that are not visible in the control force and torque produced by the velocity-feedback controller with the DQ-MEKF. They also do not appear in Fig. 5 under ideal conditions. This is expected since, unlike the DQ-MEKF, the velocity-free controller does not filter out the measurement noise nor is designed to take discrete-time measurements.

Hence, in this particular scenario, and assuming the computational resources allow it, the velocity-feedback controller in

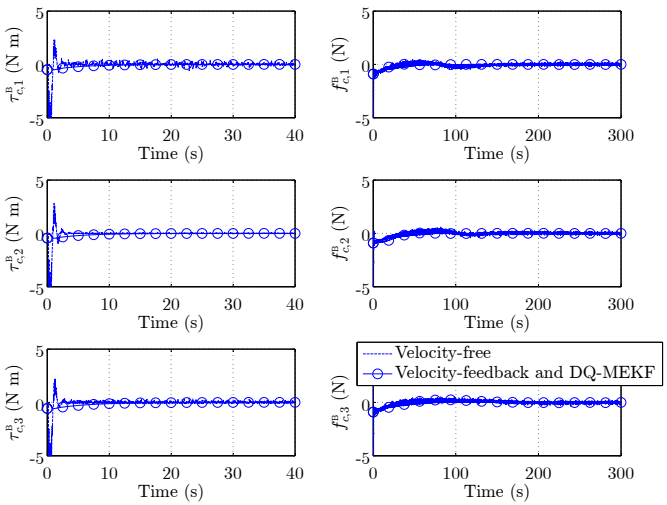

Fig. 10. Control force and torque using the velocity-free controller and the velocity-feedback controller with the DQ-MEKF.

series with the DQ-MEKF seems to be the more numerically robust solution to the pose-tracking problem without relative linear and angular velocity measurements. The velocity-free controller may be more suitable for small cheap satellites where operational requirements are not stringent and the on-board computational resources are limited.

VI. Conclusion

This paper proposes a pose-tracking controller that guarantees almost global asymptotic stability of the pose-tracking error even when relative linear and angular velocity measurements are not available. This property is proven for any reference pose with finite velocities and accelerations. The derivation of this controller is based on an existing attitude-tracking controller that guarantees almost global asymptotic stability of the attitude-tracking error when angular velocity measurements are not available and on the dual quaternion formalism. The proposed controller is specially suited for uncooperative satellite proximity operations where the only relative measurements the chaser satellite has access to are relative pose measurements from, e.g., a vision-based sensor. The proposed controller is also useful in the case of a malfunction of a velocity sensor. The simulation results presented in this paper show that in a conceivable satellite proximity operations scenario, the proposed velocity-free controller would only require 3% more ΔV than a controller that knows the true relative velocities. The simulation results presented in this paper also show that, whereas using an EKF with a velocity-feedback controller can lead to better transient responses and controls than with the velocity-free controller (at least when the measurement noise is not carefully filtered in the latter solution), the additional 84 states required by the former solution might make the velocity-free controller a better option for satellites with limited computational resources.

Acknowledgment: The authors are grateful to the reviewers for insightful comments. Support for this award has been provided by AFRL award FA9453-13-C-0201 and NSF award NRI-142645.

References

[1] P. Singla, K. Subbarao, and J. L. Junkins, "Adaptive output feedback control for spacecraft rendezvous and docking under measurement uncertainty," *Journal of Guidance, Control, and Dynamics*, vol. 29, no. 4, pp. 892–902, July-August 2006.

[2] S. Tanygin, "Generalization of adaptive attitude tracking," in *AIAA/AAS Astrodynamics Specialist Conference and Exhibit*, no. AIAA 2002-4833, Monterey, California, August 5-8 2002.

[3] H. Wong, H. Pan, and V. Kapila, "Output feedback control for spacecraft formation flying with coupled translation and attitude dynamics," in *Proceedings of the 2005 American Control Conference*, vol. 4, Portland, OR, USA, June 8-10 2005, pp. 2419–2426.

[4] D. H. S. Maithripala, J. M. Berg, and W. P. Dayawansa, "Almost-global tracking of simple mechanical systems on a general class of Lie groups," *IEEE Transactions on Automatic Control*, vol. 51, no. 1, pp. 216–225, January 2006.

[5] S. P. Bhat and D. S. Bernstein, "A topological obstruction to continuous global stabilization of rotational motion and the unwinding phenomenon," *Systems & Control Letters*, vol. 39, no. 1, pp. 63 – 70, January 28 2000.

[6] N. Filipe and P. Tsiotras, "Rigid body motion tracking without linear and angular velocity feedback using dual quaternions," in *European Control Conference*. Zürich, Switzerland: IEEE, Piscataway, NJ, July 17-19 2013, pp. 329–334.

[7] ——, "Adaptive position and attitude-tracking controller for satellite proximity operations using dual quaternions," *Journal of Guidance, Control, and Dynamics*, vol. 38, pp. 566–577, 2015, DOI: 10.2514/1.G000054.

[8] N. Filipe, M. Kontitsis, and P. Tsiotras, "Extended Kalman filter for spacecraft pose estimation using dual quaternions," *Journal of Guidance, Control, and Dynamics*, 2015, DOI: 10.2514/1.G000977.

[9] M. R. Akella, "Rigid body attitude tracking without angular velocity feedback," *Systems & Control Letters*, vol. 42, no. 4, pp. 321–326, April 6 2001.

[10] N. Filipe, "Nonlinear pose control and estimation for space proximity operations: An approach based on dual quaternions," Ph.D. dissertation, Georgia Institute of Technology, 2014. [Online]. Available: http://hdl.handle.net/1853/53055

[11] W. Haddad and V. Chellaboina, *Nonlinear Dynamical Systems and Control: A Lyapunov-Based Approach*. Princeton University Press, 2008.

[12] N. Filipe and P. Tsiotras, "Simultaneous position and attitude control without linear and angular velocity feedback using dual quaternions," in *American Control Conference*. Washington, DC: IEEE, Piscataway, NJ, June 17-19 2013, pp. 4815–4820.

[13] J. T.-Y. Wen and K. Kreutz-Delgado, "The attitude control problem," *IEEE Transactions on Automatic Control*, vol. 36, no. 10, pp. 1148–1162, October 1991.

[14] F. Lizarralde and J. T. Wen, "Attitude control without angular velocity measurement: A passivity approach," *IEEE Transactions on Automatic Control*, vol. 41, no. 3, pp. 468–472, March 1996.

[15] R. Zanetti, M. Majji, R. H. Bishop, and D. Mortari, "Norm-constrained Kalman filtering," *Journal of Guidance, Control, and Dynamics*, vol. 32, no. 5, pp. 1458–1465, September-October 2009.

Nuno Filipe is a Guidance and Control Engineer in the NASA/Caltech Jet Propulsion Laboratory. Previously, he was a Research and Teaching Assistant at the School of Aerospace Engineering (2010-2015) of the Georgia Institute of Technology (GIT) and a National Trainee at the Control Systems Division of the European Space Agency (2008-2010). Nuno Filipe has a Ph.D. in Aerospace Engineering from the GIT, a M.Sc. in Aerospace Engineering from the Delft University of Technology, and a 5-year undergraduate degree in Aerospace Engineering from Instituto Superior Técnico, Portugal. He is a recipient of the 2010-2013 International Fulbright Science and Technology Award and of the 2013 Best Graduate Student Technical Paper Award by the AIAA Guidance, Navigation, and Control Technical Committee. His Ph.D. thesis, entitled "Nonlinear Pose Control and Estimation for Space Proximity Operations: An Approach Based on Dual Quaternions" was selected as one of the 10 best of 2014 from the GIT.

Alfredo Valverde is a Ph.D. student in the School of Aerospace Engineering at the Georgia Institute of Technology (GIT). His current research lies in the field of nonlinear control and estimation. He received his B. Sc. in Aerospace Engineering (2013) from the GIT with highest honors, while holding Research and Teaching Assistant positions in the Aerospace Engineering and Computer Science Departments. He also received his M. Sc. in Aerospace Engineering (2014) with a specialization in the field of combustion and experimental research at the Aerospace Combustion Laboratory at the GIT. He has held internship positions in the Guidance and Control Analysis group at JPL (2015), at the Département Aérodynamique, Energétique et Propulsion at ISAE-SUPAERO (2012), and is actively involved in outreach programs for the enhancement of STEM education.

Panagiotis Tsiotras is the Deans Professor in the School of Aerospace Engineering at the Georgia Institute of Technology. He received his Engineering Diploma in Mechanical Engineering from the National Technical University of Athens, in Greece (1986) and his PhD degree in Aeronautics and Astronautics from Purdue (1993). He also holds an MS degree in Mathematics from Purdue. He has held visiting research appointments at MIT, JPL, INRIA Rocquencourt, and Mines ParisTech. His main research interests are in optimal and nonlinear control, and vehicle autonomy. He has served in the Editorial Boards of the Transactions on Automatic Control, the IEEE Control Systems Magazine, the AIAA Journal of Guidance, Control and Dynamics and the journal Dynamics and Control. He is the recipient of the NSF CAREER award, and is a Fellow of AIAA and a Senior Member of IEEE.